1

New Applications of Immobilized Metal Ion Affinity Chromatography in Chemical Biology

Rachel Codd, Jiesi Gu, Najwa Ejje and Tulip Lifa
School of Medical Sciences (Pharmacology) and Bosch Institute, The University of Sydney, Australia

1.1 Introduction

Immobilized metal ion affinity chromatography (IMAC) was first introduced as a method for resolving native proteins with surface exposed histidine residues from a complex mixture of human serum [1]. IMAC has since become a routine method used in molecular biology for purifying recombinant proteins with histidine tags engineered at the *N*- or *C*-terminus. The success of IMAC for protein purification may have obscured its potential utility in other applications in biomolecular chemistry and chemical biology. Since there exists in nature a multitude of non-protein based low molecular weight compounds that have an inherent affinity towards metal ions, or that have a fundamental requirement for metal ion binding for activity, IMAC could be used to capture these targets from complex mixtures. This highly selective affinity-based separation method could facilitate the discovery of new anti-infective and anticancer compounds from bacteria, fungi, plants, and sponges. A recent body of work highlights new applications of IMAC for the isolation of known drugs and for drug discovery, metabolome profiling, and for preparing metal-specific molecular probes for chemical proteomics-based drug discovery. At its core, IMAC is a method underpinned by the fundamental tenets of coordination chemistry. This chapter will briefly focus on these aspects, before moving on to describe a number of recent innovations in IMAC. The ultimate intent of this chapter is to seed interest in other research groups for expanding the use of IMAC across chemical biology.

Inorganic Chemical Biology: Principles, Techniques and Applications, First Edition. Edited by Gilles Gasser.

1.2 Principles and Traditional Use

An IMAC system comprises three variable elements (Fig. 1.1): the insoluble matrix (green), the immobilized chelate (depicted as iminodiacetic acid, IDA, red), and the metal ion (commonly Ni(II), blue). Critical to the veracity of IMAC as a separation technique is that the coordination sphere of the immobilized metal–chelate complex is unsaturated, which allows target compounds to reversibly bind to the resin via the formation and dissociation of coordinate bonds. Each element of the IMAC system can be varied independently or in combination, which, together with basic experimental conditions (buffer selection, pH value), will influence the outcome of a separation experiment. This modular type of experimental system allows a high level of control for optimization.

In accord with its original intended use, the majority of IMAC targets are proteins, which even as native molecules can bind to the immobilized metal–chelate complex with variable affinities, as determined by the presence of surface exposed histidine residues and, in some cases, more weakly binding cysteine residues (Fig. 1.1, protein shown at left). Compared with native proteins, recombinant proteins, which feature a hexameric histidine repeat unit (His-tag) engineered at the *C*- or *N*-terminus, are higher affinity IMAC targets (Fig. 1.1, protein shown at middle). In this case, the *C*-terminal histidine residues of the recombinant protein displace the three water ligands in the immobilized Ni(II)–IDA coordination sphere, with the majority of the components in the protein expression mixture not retained on the resin (Fig. 1.2). After washing the resin to remove these unbound components, the coordinate bonds between the Ni(II)–IDA complex and the *C*-terminal histidine residues are dissociated by competition upon washing the resin with a buffer containing a high concentration of imidazole.

Phosphorylated proteins (Fig. 1.1, protein at right) as studied in phosphoproteomics [2–4], are also isolable using an IMAC format, based upon the affinity between Fe(III) and phosphorylated proteins (Fe(III)–phosphoserine, log $K \sim 13$ [5]). The IMAC-compatible metal ions most suited for phosphoproteomics include Fe(III), Ga(III), or Zr(IV), with

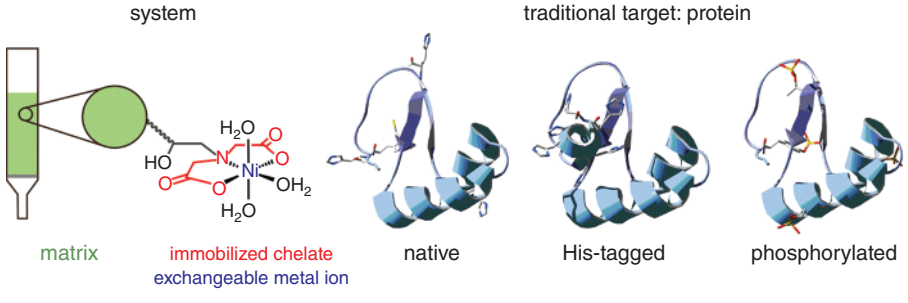

Figure 1.1 *The elements of an immobilized metal ion affinity chromatography (IMAC) experiment. The system (left-hand side) comprises an insoluble matrix (green) with a covalently bound chelate (iminodiacetic acid, IDA, red) which coordinates in a 1:1 fashion a metal ion (Ni(II), blue) to give a complex with vacant coordination sites available for the reversible binding of targets with metal binding groups. Traditional IMAC targets (right-hand side) include native proteins with surface exposed histidine residues, histidine-tagged proteins, and phosphorylated proteins*

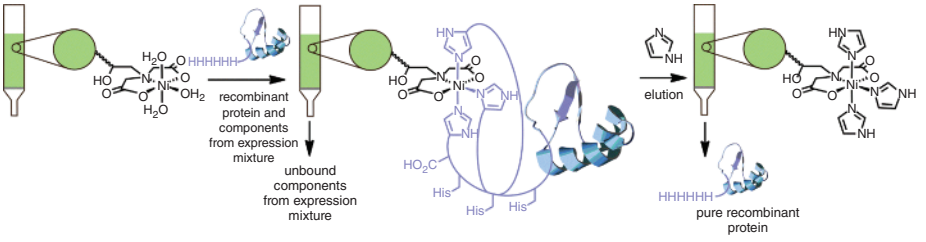

Figure 1.2 *The traditional use of IMAC for the purification of His-tagged recombinant proteins. The recombinant protein binds to the immobilized coordination complex upon the displacement of water ligands by the histidine residues engineered at the N- or C- (as shown) terminus. The resin is washed to remove unbound components from the expression mixture, and the purified protein is eluted from the resin by competition upon washing with a high concentration of imidazole buffer*

these hard acids having preferential binding affinities towards the hard base phosphate groups. This highlights that the IMAC technique is governed by key principles of coordination chemistry, including the hard and soft acids and bases (HSAB) theory [6], coordination number and geometry preferences, and thermodynamic and kinetic factors.

Because there is a significant market demand for IMAC-based separations, considerable research in the biotechnology sector has focused upon finding new and improved matrices and immobilized chelates. Common matrices include cross-linked agarose, cellulose, and sepharose. These polymers can be prepared with different degrees of cross-linking, branching, and different levels of activation, which affect the concentration of the immobilized chelate in the final matrix. There are several different types of immobilized chelates in use in IMAC applications (Fig. 1.3), with the most common being tridentate iminodiacetic acid (IDA, **A**) and tetradentate nitrilotriacetic acid (NTA, **B**). Immobilized tetradentate *N*-(carboxymethyl)aspartic acid (CM-Asp, **C**) and pentadentate *N*,*N*,*N*′-tris(carboxymethyl)ethylenediamine (TED, **D**) are used less frequently. These different *N*- and *O*-atom containing ligand types cover a range of degrees of coordinative unsaturation, which for a metal ion with an octahedral coordination preference would span: three available sites ($M(N_1O_2(OH_2)_3)$ (IDA)), two available sites ($M(N_1O_3(OH_2)_2)$ (NTA), $M(N_1O_3(OH_2)_2)$ (CM-Asp)), and one available site ($M(N_2O_3(OH_2))$ (TED)). A significant number of resins with non-traditional immobilized chelates, such as 1,4,7-triazocyclononane [7], 8-hydroxyquinoline [8] or *N*-(2-pyridylmethyl)aminoacetate [9] have been prepared, which have different performance characteristics with respect to protein purification, compared with the traditional IMAC resins.

The nature of the immobilized coordination complex, in terms of both chelate and metal ion, has a major influence on the outcome of an IMAC procedure. An example of the influence of the chelate is found in early studies, which focused on the development of IMAC for phosphoproteomics. Fractions of phosphoserine-containing ovalbumin were retained on an immobilized Fe(III)–IDA resin, but were not retained on an immobilized Fe(III)–TED resin [2]. While an explanation for this observation was not provided in the original work, we posit that this is most likely due to the difference between the number of available coordination sites in the Fe(III)–IDA complex (three sites) and the Fe(III)–TED complex (one site) (Fig. 1.3). This would suggest that retention of ovalbumin fractions via phosphoserine

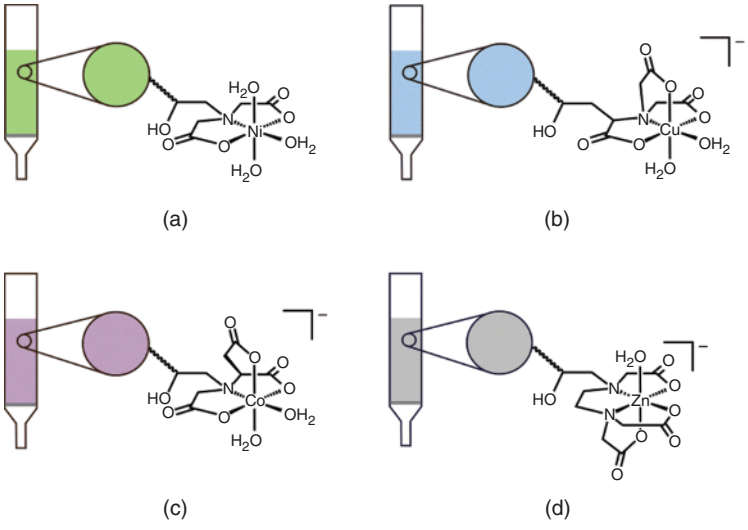

Figure 1.3 *Immobilized chelates used in IMAC applications. Chelates: iminodiacetic acid (IDA, a), nitrilotriacetic acid (NTA, b), N-(carboxymethyl)aspartic acid (CM-Asp, c) or N,N,N′-tris(carboxymethyl)ethylenediamine (TED, d). A range of metal ions, including Ni(II), Cu(II), Co(II) or Zn(II), are compatible with each type of immobilized chelate. The type of chelate and the coordination preferences of the metal ion will direct the degree of coordinative unsaturation of the immobilized complex*

residues involves at least a bidentate binding mode, and that the single coordination site at the Fe(III)–TED complex was insufficient for retaining the target.

1.3 A Brief History

As an enabling technology, IMAC has played a significant role in accelerating knowledge of molecular, cell, and human biology, through expediting access to significant quantities of pure proteins. For a technique that is conducted every day in many laboratories around the world, it is interesting to reflect briefly upon the history and acceptance of IMAC in its early phases of development. The many review articles available on the history of IMAC [10–14] warrants only a brief coverage of this topic here. The first description of IMAC for protein fractionation used Zn(II)- or Cu(II)-loaded IDA resins prepared in house, with the columns configured in series [1]. Processing of an aliquot of human serum showed that the Zn(II) column was enriched with transferrin, acid glycoprotein, and ceruloplasmin, while the Cu(II) column was enriched with albumin, haptoglobins and β-lipoprotein [1]. In the ten years following this initial report, aside from sporadic reports of IMAC formats using immobilized Cd(II), Ca(II) or Cu(II), the dominant IMAC format in use for protein separation was Zn(II)–IDA, which had mixed success. In its infancy, IMAC gathered only modest traction in the protein purification research community. The uptake of IMAC improved after a follow up study from the initial authors, which highlighted its broad utility [15]. In this second report, the use of Ni(II)- or Fe(III) loaded IDA resin was described, together

with a TED-immobilized resin loaded with these same metal ions, which performed well in purifying native proteins with surface exposed histidine residues. Nickel(II)–IDA resin ultimately became the IMAC format of choice for many protein-based applications [16].

The exponential rise in the use of IMAC came with the demonstration of its utility for purifying recombinant proteins [17]. His-tagged protein constructs were isolated from complex mixtures using an Ni(II)–IDA (Fig. 1.2) or –NTA resin with extraordinary selectivity. The dovetailed techniques of recombinant molecular biology and IMAC guaranteed the rapid uptake of IMAC in life science research laboratories and spurred high activity in IMAC-related product development in biotechnology companies, which continues today. Both the lag time and eventual traction of IMAC is evident from a plot of the number of citations per year of the article first reporting its use for native proteins [1], and of the article that described its use for recombinant protein purification [17] (Fig. 1.4).

1.4 New Application 1: Non-protein Based Low Molecular Weight Compounds

Since many non-protein based low molecular weight compounds have an inherent affinity to metal ions, or have a fundamental requirement for metal ion binding for activity, IMAC could have potential for isolating these types of compounds. This could expedite natural products based drug discovery, because secondary metabolites in bacterial culture or extracts from plants and marine life are usually present in very small quantities and require careful purification to provide sufficient yields for downstream structural characterisation and biological screening [18]. As an affinity-based separation method, IMAC has particular value in this regard, since the target material can potentially be concentrated

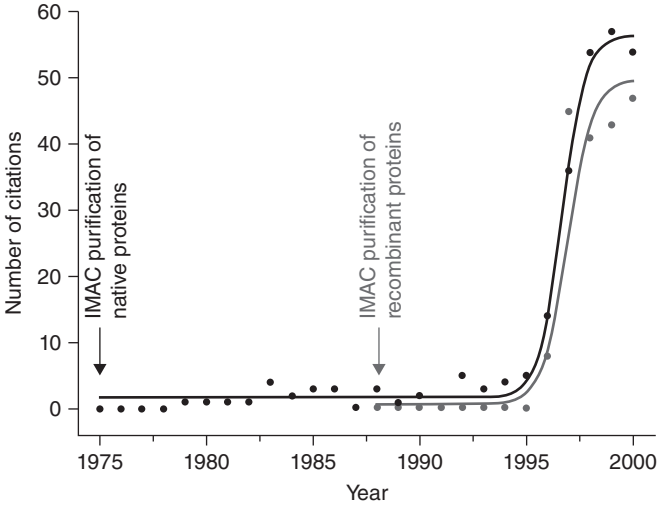

Figure 1.4 *Citations per year for the publications that first described IMAC for native protein purification (black) [1] and that first used IMAC for Hig-tag recombinant protein purification (grey) [17]. There was a 20-year lag time between the discovery of IMAC and its wide acceptance as a powerful method for the purification of recombinant proteins*

on the resin from large volumes of native dilute culture or extract, thereby circumventing concentration steps often necessary in more traditional purification protocols. To test the veracity of using IMAC for purifying non-protein based low molecular weight targets, our group selected bacterial siderophores as a test construct.

1.4.1 Siderophores

Our laboratory has a significant focus on research into the chemical biology of siderophores, which are low molecular weight ($M_r \sim 1000\,g\,mol^{-1}$) organic chelates produced by bacteria for the purpose of Fe acquisition [19–25]. Under aqueous, pH neutral, and aerobic conditions, most Fe is present as insoluble Fe(III)–oxyhydroxide species, which restricts its availability to bacteria through passive uptake. In response to this environmental challenge, bacteria have evolved a number of mechanisms to guarantee supply of essential Fe, with the production of Fe(III)-specific siderophores as one of the most successful and widespread of these adaptations. Siderophores excreted by bacteria into the extracellular milieu solubilize local Fe(III) in soil, or in Fe-bound proteins such as transferrin in a mammalian host, to form stable Fe(III)–siderophore coordination complexes. The Fe(III) is returned to the bacterial cell through a protein-mediated cascade, which is initiated by an avid recognition event between the Fe(III)–siderophore complex and cell-surface receptors of the source bacterium. Ultimately, the Fe(III)–siderophore complex is dissociated in the cytoplasm to liberate Fe for incorporation into the multiple Fe-containing proteins, including cytochromes, ribonucleotide reductase and aconitase, which are fundamental for life [26, 27].

By virtue of their ability to coordinate Fe(III) with high affinity, and a range of other metal ions with lower affinity [28], siderophores have potential in treating metal ion mediated pathologies in humans, and have applications in environmental metal remediation [28–36]. Owing to the bacterial competition for limited Fe, it is often the case that a bacterial genome will code for the biosynthesis of a structurally unique siderophore that is recognized as the Fe(III)-loaded complex by a structurally unique cell receptor. Both the structural diversity and the breadth of metal binding applications in the areas of health and the environment fuel research towards building a comprehensive library of siderophores across the bacterial kingdom.

As is common to most targets in natural products, siderophores are produced in native cultures in very small quantities ($<1\,mg\,L^{-1}$) [37, 38], which limits the ability to obtain sufficient amounts for structural characterisation using spectroscopy and X-ray crystallography. This limitation led us to consider more streamlined approaches to purifying siderophores from complex bacterial culture medium, with the aim of delivering a robust separation method that would facilitate siderophore profiling. Siderophores have been classified into three groups, based upon the nature of the Fe(III) binding groups: hydroxamic acids, catechols, or hydroxycarboxylic acids, with the last class being based on citric acid scaffolds [39]. The metal binding ability inherent to siderophores prompted us to consider whether IMAC could be used to select these ligands from a bacterial culture. Our first experiments in this regard focused upon the hydroxamic acid based siderophore, desferrioxamine B (DFOB), which is produced by the non-pathogenic soil bacterium *Streptomyces pilosus*. The mesylate salt of DFOB is used to treat, via sub-cutaneous infusion,

secondary iron overload disease, which arises from the frequent blood transfusions necessary to prevent life-threatening anaemia symptomatic of genetic blood disorders, including beta-thalassaemia and myelodysplastic syndromes [40–42]. Despite the release of new orally-active synthetic iron chelating agents for these conditions, including deferasirox and deferiprone [40], DFOB remains the "gold standard" for iron overload disease, due to its high affinity towards Fe(III) and its low toxicity for chronic use.

The high affinity of siderophores towards Fe(III), prompted caution about using Fe(III)–IDA IMAC resins for their separation, since it would be likely that the siderophore (Fe(III)–DFOB, log *K* 30.6) would compete against the IDA (Fe(III)–IDA, log *K* 10.7) for Fe(III) and strip it from the resin, thereby providing no resolution from the bulk mixture (Table 1.1).

One report described the isolation of siderophores from *Alcaligenes eutrophus* CH34 using Fe(III)-based IMAC [46]. *A. eutrophus* CH34 was subsequently renamed *Ralstonia eutropha* CH34 and is known presently as *Cupriavidus metallidurans* CH34. The compound that gave a positive result in the universal siderophore chrome azurol sulfonate (CAS) detection assay, was identified in the original report as a hydroxamic acid based siderophore [46], subsequently as a novel phenolate-based siderophore (M_r 1.470 g mo1^{-1}) that contained neither hydroxamic acid nor catecholate groups [47], and finally by other workers using chemical degradation and spectroscopy, as the citric acid based siderophore staphyloferrin B [48]. In the initial report, the reduced affinity between Fe(III) and a hydroxycarboxylate-based siderophore [49], as distinct from a hydroxamic acid based siderophore, may have enabled the use of Fe(III)-based IMAC purification, although this method was not used for the isolation of this siderophore beyond the first report.

In our studies, we chose to use Ni(II)-based IMAC to examine the ability of the method to select for DFOB from bacterial culture (Fig. 1.5). The Ni(II)–DFOB affinity constant

Table 1.1 *Equilibrium constants for metal complexes formed with immobilized ligands relevant to IMAC and selected non-protein based low molecular weight molecular targets*

Ligand	Abbrev.	Equilibrium	Log $K^{a,b}$					
			Fe(III)	Co(II)	Ni(II)	Cu(II)	Zn(II)	Yb(III)
Iminodiacetic acid	IDA	ML/(M · L)	10.7[c]	6.9	8.1	10.6	7.2	7.4
N-methyliminodiacetic acid	MIDA	ML/(M · L)	NA[e]	7.6	8.7	11.0	7.6	7.6
Nitrilotriacetic acid	NTA	ML/(M · L)	15.9	10.4	11.5	12.9	10.7	12.2
		$ML_2/(M \cdot L)^2$	24.3[d]	14.3	16.3	17.4	14.2	21.4[b]
Ethylenediaminetetraacetic acid	EDTA	ML/(M · L)	25.0	16.3	18.5	18.7	16.4	19.5
Acetohydroxamic acid	AHA	ML/(M · L)	11.4[d]	5.1[d]	5.3[d]	7.9[d]	5.4[d]	6.6[d]
Desferrioxamine B	DFOB	MHL/(M · HL)	30.6[d]	10.3[d]	10.9[d]	14.1[d]	10.1[d]	16.0[d]
Desferrioxamine E	DFOE	ML/(M · L)	32.5[d]	11.9[d]	12.2[d]	13.7[d]	12.1[d]	NA[e]
Bleomycin A_2	$BLMA_2$	ML/(M · L)	NA[e]	9.7[d, f]	11.3[d, f]	12.6[d, f]	9.1[d, f]	NA[e]

[a] 25 °C, 0.1 M (unless specified otherwise).
[b] From References 43 and 44 (unless specified otherwise).
[c] 25 °C, 0.5 M.
[d] 20 °C, 0.1 M.
[e] NA, not available.
[f] From Reference 45.

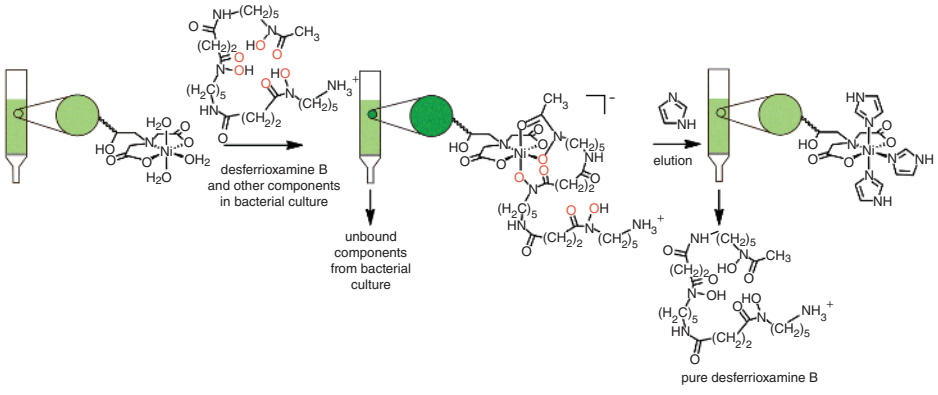

Figure 1.5 *A new use of IMAC for the purification of bacterial secondary metabolites with metal ion binding affinity, such as desferrioxamine B (DFOB). In a fashion similar to its traditional use (refer to Fig. 1.2), the target low molecular weight non-protein based metabolite binds to the immobilized coordination complex upon the displacement of water ligands by the metal binding functional groups (for DFOB, hydroxamic acid groups). The resin is washed to remove unbound components from the bacterial culture supernatant and the purified metabolite is eluted from the resin by competition upon washing with a high concentration of imidazole buffer, or by decreasing the pH value of the elution buffer to pH < pK_a (functional group). The figure shows a posited binding mode between analyte and resin*

(log *K* 10.9) foreshadowed that compared with Fe(III)–IDA based IMAC, DFOB would have a reduced propensity to leach Ni(II) from the Ni(II)–IDA complex. This would manifest as a binding event between DFOB and the immobilized Ni(II)–IDA complex, rather than elution of Ni(II)-loaded DFOB. Several reports of Ni(II)–hydroxamic acid coordination chemistry suggested that Ni(II) might be a judicious choice of metal ion [50–52].

These experiments showed that a 1 mL column of Ni(II)–IDA resin bound about 350 nmol of the monohydroxamic acid acetohydroxamic acid at pH 9.0, and, that under the same conditions, the binding capacity of the resin increased to about 3000 nmol for the dihydroxamic acid suberodihydroxamic acid and the trihydroxamic acid DFOB, which correlated with available stability constants [53], and reflected the potential ability of the latter two ligands to act as at least tridentate ligands towards the resin for improved binding. The optimal pH value for binding these hydroxamic acid standards was pH 9, which is close to the pK_a value of the N–OH proton in aqueous solvents [54]. At higher pH values, metal hydroxides can precipitate on the resin. Most striking about this study was the selection of native DFOB from a crude culture supernatant of *S. pilosus* [55]. This crude culture supernatant was not subject to any pre-treatment steps, aside from adjusting the pH value to 9.0. As evident from the HPLC (high-performance liquid chromatography) trace (Fig. 1.6, A), the crude mixture contained many components, including those from the bacteriological medium (amino acids, peptides, vitamins) and other secondary metabolites produced by *S. pilosus*. Single-step processing using Ni(II)-based IMAC selected five major components from the mixture, with two components co-eluting under the peak at $t_R = 8.9$ min (Fig. 1.6, B). Based on mass spectrometry and the use of samples spiked with authentic DFOB, the peaks at t_R = 15.03 and 15.45 min (B, boxed) were ascribed to $DFOA_1$ and DFOB, respectively,

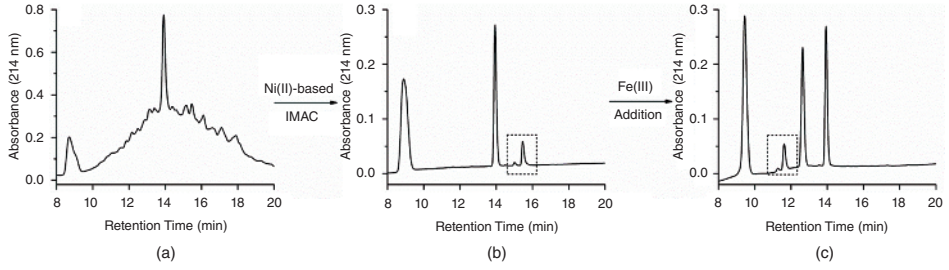

Figure 1.6 *Crude S. pilosus culture, which contained many components as measured by RP-HPLC (a), was processed using Ni(II)-based IMAC to select for DFOB (major) and $DFOA_1$ (minor) as metal free (b, boxed) and Fe(III)-loaded (c, boxed) species. The IMAC process selected five components from the complex mixture, which were more completely resolved upon the addition of Fe(III). Compared with the free ligands, Fe(III)-loaded DFOB and $DFOA_1$ eluted on the RP-HPLC column in a window described by increased water solubility, which is consistent with the role of siderophores to increase the water solubility of Fe(III). Adapted with permission from [55] © 2008 Royal Society of Chemistry*

from the ferrioxamine class of siderophores [19, 20, 56]. In the presence of added Fe(III), these peaks (C, boxed) shifted in a systematic fashion to a more hydrophilic region of the reverse-phase HPLC (RP-HPLC) trace, in accord with the role of siderophores to increase the water solubility of Fe(III). The LC–MS (liquid chromatography–mass spectrometry) data from the Fe(III)-loaded solution correlated with the identification of Fe(III)–$DFOA_1$ and Fe(III)–DFOB. The signals at $t_R = 9.45$, 12.63, and 13.93 min (C) were derived from components in the medium, and showed variable Fe(III) responsiveness.

This work demonstrated the potential of IMAC for selecting clinically valuable agents direct from bacterial culture. Nickel(II)-based IMAC would be predicted to be useful in the isolation of other types of siderophores, including but not limited to, the catecholate-based compounds enterobactin or salmochelin from *Escherichia* species, the 2-hydroxyphenyloxazoline ring-based siderophores from *Mycobacteria* [57], and marine siderophores, such as lystabactin [58]. Recent compendiums of the full structural diversity of siderophores [19, 20] provide a range of promising IMAC-compatible targets.

The metal ion selected for the IMAC procedure has a major influence on the experimental outcome. As predicted, Fe(III)-loaded IMAC resin was not suitable for the capture of high affinity Fe(III) binding hydroxamic acid based siderophores. In this case, the DFOB sequestered the Fe(III) from the immobilized Fe(III)–IDA complex (Equation 1.1, log *K* 19.9) and was eluted in the wash fraction as the Fe(III)-loaded complex (Fig. 1.7, A). In the case of Ni(II)-based IMAC, the respective Ni(II)–DFOB and Ni(II)–IDA affinity constants (Table 1.1) were better poised to enable successful product retention (Equation 1.2, log *K* 2.8) and elution of DFOB in a metal-free form (Fig. 1.7, B).

$$[Fe(III)(IDA)(OH_2)_3]^+ + DFOBH_4^+ \rightleftharpoons [Fe(III)(DFOBH)]^+ + IDAH_2 + 3H_2O + H^+ \quad (1.1)$$

$$[Ni(II)(IDA)(OH_2)_3] + DFOBH_4^+ \rightleftharpoons [Ni(II)(DFOBH)] + IDAH_2 + 3H_2O + H^+ \quad (1.2)$$

In other experiments, V(IV)-loaded IDA resin was prepared with the intent of capturing DFOB. While DFOB and related hydroxamic acids have a rich coordination chemistry

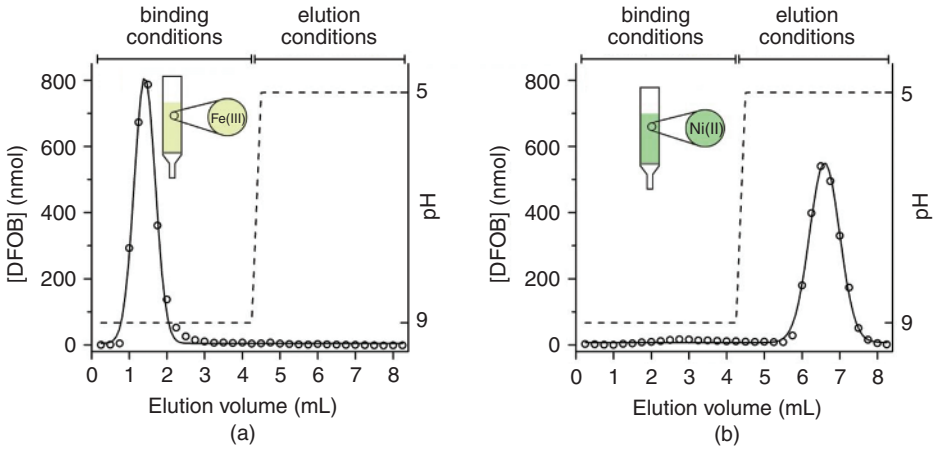

Figure 1.7 *The performance of Fe(III)- (a) or Ni(II)- (b) based IMAC for targeting desferrioxamine B (DFOB) purification. In the case of Fe(III)-based IMAC, DFOB out-competed IDA for Fe(III) (refer to Equation 1.1), and was eluted from the resin as unbound Fe(III)-loaded DFOB. In the case of Ni(II)-based IMAC, the competition between DFOB and IDA for Ni(II) (refer to Equation 1.2) was poised in a region that effected DFOB binding to the resin at pH 9, with its subsequent elution as the metal free ligand at pH 5*

with V(IV) and V(V) [38, 59–64], DFOB was not retained on this resin. This is probably attributable to the insufficient number of available coordination sites on the immobilized [V(IV)(O)(IDA)] complex. A similar rationale would suggest that V(V)-loaded IDA resins containing the immobilized $[V(V)(O)_2(IDA)]^-$ complex would be close to coordinatively saturated and prevent ligand binding.

1.4.2 Anticancer Agent: Trichostatin A

The enzyme-mediated modification of chromatin is at the forefront of cancer research, since the topology of this protein (histone)–polynucleotide structure directs transcriptional activity [65]. A common modification to the histone component of chromatin is the *N*-acetylation of selected lysine residues, with the acetylation status controlled by a two-enzyme system: the histone acetyltransferases (HATs) and the histone deacetylases (HDACs). Upregulated HDAC activity leads to a higher concentration of unmasked lysine residues, which causes chromatin to condense into a less transcriptionally active form, which in turn attenuates the expression of tumor suppressor genes. The gene silencing effects of upregulated HDAC activity is associated with the onset and progression of cancer, with this class of enzyme validated as an anticancer target [66, 67]. Three of the four classes of the 18 known HDAC isoforms are Zn(II)-containing enzymes, which render Zn(II) binding compounds as potential HDAC inhibitors [68–72].

One of the most potent inhibitors of Zn(II)-containing HDACs is the monohydroxamic acid trichostatin A (TSA), which was discovered from cultures of *Streptomyces hygroscopicus* Y-50 [73]. TSA (HDAC1, $IC_{50} \sim 5$ nM [74]) has served as a lead compound for designing inhibitors against HDACs and other disease relevant Zn(II)-containing enzymes, including matrix metalloproteinases, metallo-β-lactamases, carboxypeptidase A,

and carbonic anhydrase [28, 30, 75–78]. The structurally simpler TSA analogue suberoylanilide hydroxamic acid (SAHA, vorinostat) inhibits HDACs through Zn(II) coordination [79] and is in clinical use for the treatment of cutaneous T cell lymphoma. Studies of the coordination chemistry of SAHA with metals including Ni(II) [80] and the experiments that showed acetohydroxamic acid bound to Ni(II)–IDA resin [55], prompted studies to establish the utility of IMAC for isolating TSA from culture. IMAC also had the potential to resolve mixtures of TSA and the β-glucosyl-substituted analogue trichostatin C (TSC). TSA is a costly chemical and can be prepared in its enantiomeric pure form (99% e.e.) using total synthesis only on a small scale [81]. The ability to access TSA and other analogues from culture would be valuable for drug discovery and for the fine chemicals industry.

A standard solution of TSA bound to Ni(II)–IDA resin at a loading of 0.5 μmol mL^{-1} with recovery at >95%. The capacity of the Ni(II)–IDA resin towards binding TSA from the culture of native TSA- and TSC-producing *Streptomyces hygroscopicus* MST-AS5346 was reduced, due to the presence of competing ligands, including those present in the culture medium and other secondary metabolites with inherent metal binding affinity [82]. In the native culture, there were at least 50 species detected by UV spectroscopy (ultraviolet) (Fig. 1.8, A) and 150–200 species detected using LC–MS in the total ion current (TIC) mode. The presence of TSA, TSC, and trichostatic acid, the last of which is both a TSA precursor and hydrolysis product, was confirmed from LC–MS measurements. The

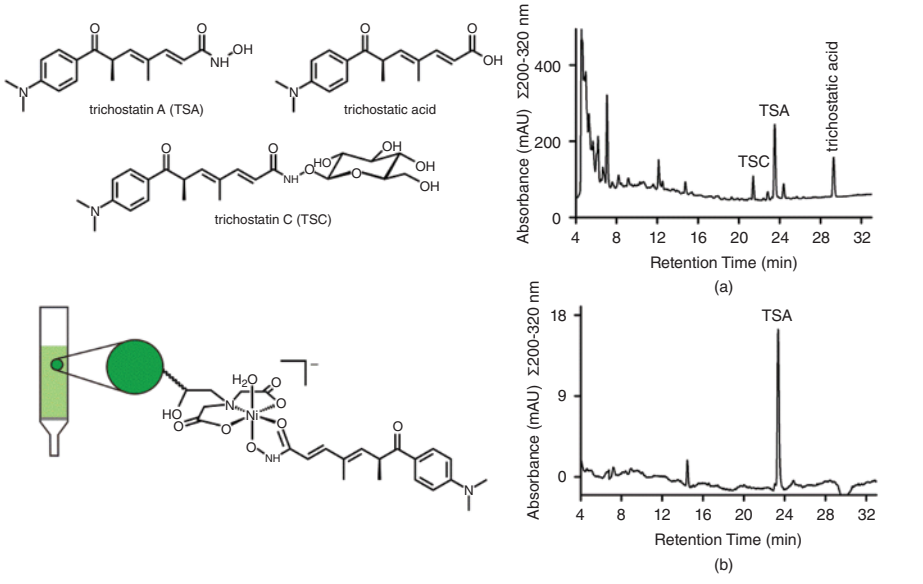

Figure 1.8 *Nickel(II)-based IMAC for the purification of trichostatin A (TSA) from Streptomyces hygroscopicus MST-AS5346 culture, with a posited binding mode between analyte and resin shown at the lower left. As determined by RP-HPLC, this method was effective at resolving TSA (B) from a complex mixture of components, including TSA, the –NH-O-glycosyl analogue TSC and trichostatic acid (A), present in the bacterial culture supernatant. Adapted with permission from [82] © 2012 Royal Society of Chemistry*

fraction containing unbound components was enriched with TSC and trichostatic acid, in addition to containing about 20% of the total TSA. The glucose masked NH–O group of TSC and the terminal carboxylic acid group of trichostatic acid prevented these compounds binding to the resin. The bound component was enriched with TSA (Fig. 1.8, B), with the method showing striking selectivity towards capturing TSA above TSC and trichostatic acid. A minor species in the bound fraction was detected at t_R 14.5 min (m/z_{obs} 432.89), which was not identified, but could be a potential inhibitor of Zn(II)- or Ni(II)-containing metalloproteins.

1.4.3 Anticancer Agent: Bleomycin

Bleomycins are a family of glycopeptide antibiotics produced by *Streptomyces verticillus* that are used clinically to treat a number of cancers [83–85]. Combination therapy of bleomycin, cisplatin, and etoposide has contributed to an increase to 90% in the cure rate of testicular cancer [86]. The total synthesis of bleomycin has been achieved [87], but for pharmaceutical-scale production, it is purified from large-scale *S. verticillus* fermentation broths. The structural elements of bleomycin include a metal-binding region, comprised of nitrogen donor atoms from imidazole, β-hydroxyhistidine (amide), pyrimidine, and β-aminoalanine (primary and secondary amines) [88–90], a bithiazole group with pendant groups that distinguish between different bleomycin congeners, and a disaccharide motif [84, 85]. The coordination of Fe(II) to the metal-binding region of bleomycin is integral to its mechanism of action, with the ultimate production of a low-spin ferric peroxide species (O_2^{2-}–Fe(III)–bleomycin) that cleaves DNA [91–93]. During fermentation, the metal binding region of bleomycin selects for Cu(II) (log K 12.6) (Table 1.1), which needs to be removed from the complex prior to clinical use.

Since bleomycin has a natural affinity towards Cu(II), we undertook to establish the efficacy of Cu(II)-based IMAC for bleomycin purification. Similar to the approaches taken for the isolation of DFOB and TSA, we began by optimizing the capture of a standard solution of bleomycin on Cu(II)–IDA resin, which showed a binding capacity of 300 nmol mL^{-1} [94]. In experiments aimed to select bleomycin directly from *S. verticillus* culture, the endogenous Cu(II) was first removed by adsorbing the culture onto a macroreticular XAD-2 resin and washing the resin with EDTA, similar to the process used industrially. After this process, the Cu(II)-free mixture was loaded at pH 9 onto the Cu(II)-loaded IMAC resin. Similar to the previous examples, compared with a standard bleomycin solution, the capture of bleomycin from culture was less efficient, with about 50% capture, due to the presence of competing ligands in the complex mixture. The crude XAD-2 treated culture contained at least 50 UV-active species (Fig. 1.9, A). The majority of these species appeared in the unbound fractions, with the two dominant bleomycin congeners, bleomycin A_2 ($BLMA_2$) and bleomycin B_2 ($BLMB_2$), appearing in the fractions collected under elution conditions (Fig. 1.9, B). The purification factor for the resolution of $BLMA_2$ and $BLMB_2$ from the bulk mixture was conservatively estimated as 25. The affinity of $BLMB_2$ towards the Cu(II)–IDA complex was somewhat greater than in the case of $BLMA_2$, with a higher proportion of the latter congener appearing in the wash fraction, and a higher proportion of the former congener appearing in the elution fraction. Since the primary metal binding region of $BLMA_2$ and $BLMB_2$ is the same, the difference in binding to the Cu(II)–IDA resin

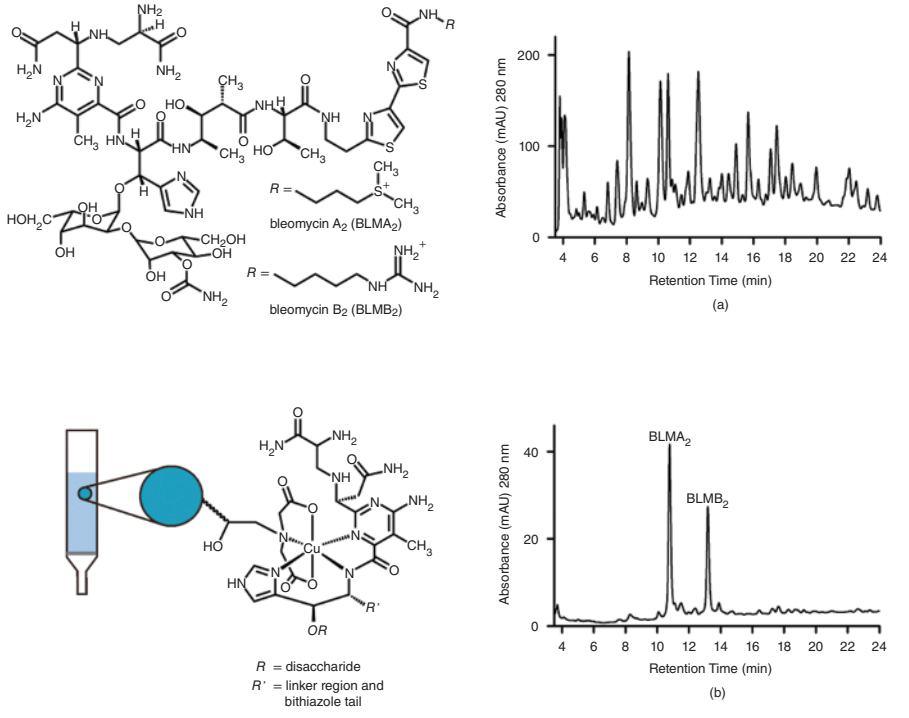

Figure 1.9 *Copper(II)-based IMAC for the purification of bleomycin from Streptomyces verticillus culture, with a posited binding mode between analyte and resin shown at the lower left. As determined by RP-HPLC, this method was effective at resolving the two major bleomycin congeners $BLMA_2$ and $BLMB_2$ (b) from a complex mixture of components (a) present in the bacterial culture supernatant. Reprinted with permission from [94] © 2012 Elsevier*

must be attributable to the bithiazole-substituted group. In the case of $BLMB_2$, a coordinate bond between Cu(II) and an agmatine-based nitrogen atom might be possible, similar to the observed binding between arginine or agmatine and the Mn(II)-containing enzymes arginase [95] or agmatinase [96], respectively. This additional interaction could result in a stronger interaction with the Cu(II)–IDA resin, as observed experimentally. Together with the studies of the selection of DFOB or TSA from crude culture medium, the experiments using bleomycin support the utility of IMAC for the streamlined capture of metal binding pharmaceutical agents.

1.4.4 Anti-infective Agents

The use of IMAC for isolating non-protein based pharmaceutical agents has been garnering increased research interest. A recent study determined the utility of Cu(II)- and Fe(III)-based IMAC for analyzing antibiotic drugs in veterinary and human use [97]. The study showed that solutions from standard samples of tetracycline-, fluoroquinoline-, macrolide-, aminoglycoside-, and β-lactam-based antibiotics were adsorbed with significant recoveries on both Cu(II)- and Fe(III)-loaded IMAC resins, and that sulfonamides and steroid- and non-steroid hormones were not retained. An examination of the structures

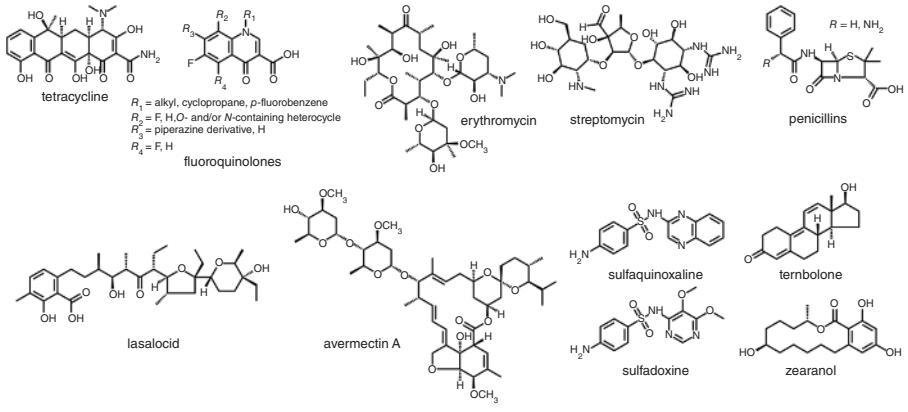

Figure 1.10 *Antibiotic compounds and veterinary anti-parasitic compounds and hormones examined as IMAC targets. The agents that bound to Cu(II)- or Fe(III)-loaded resins have functional groups configured to form coordination complexes compatible with IMAC processing*

of each of these compounds informs the experimental results (Fig. 1.10). The antibiotic components that were retained on IMAC resins have multiple oxygen and/or nitrogen donor atoms configured to form stable five- or six-membered chelate rings with the immobilized Cu(II)- or Fe(III)-IDA complex: tetracycline (keto, carboxamide, vicinal diol), fluoroquinolines (keto, carboxylate), erythromycin (vicinal diol), streptomycin (vicinal diol, α-hydroxycarboxylate, amine), and penicillins (amide, carboxylate). Each of these antibiotics has been discussed in the coordination chemistry literature [98, 99], which is a useful indicator of the veracity of using IMAC for their isolation. Components that showed minimal (lasalocid, avermectin A) or no retention (sulfonamides, trenbolone, zearanol) on the IMAC resin had insufficient and/or poorly configured donor groups for coordination. While close to 100% of the penicillin-based antibiotic ampicillin (R = NH_2) was retained on both the Cu(II)- and Fe(III)-loaded IMAC resin, only 70% of benzylpenicillin (R = H) was retained on the Fe(III)-loaded resin, and only 35% of the sample was retained on the Cu(II)-loaded resin. This is probably due to the amino nitrogen atom and carbonyl oxygen atom of the amide group of ampicillin being correctly configured to furnish a stable five-membered coordination ring with the immobilized Cu(II)– or Fe(III)–IDA complex. The significant difference in binding phenomenon between these two closely related compounds illustrates the influence of coordination chemistry in selecting suitable targets for IMAC purification. In the case of β-lactam antibiotics, the use of Zn(II)- or Co(II)-loaded resins could lead to the metal ion catalyzed hydrolysis of the β-lactam ring, which would yield ring opened structures upon elution [100].

1.4.5 Other Agents

Copper(II)-loaded IDA resins have been used to concentrate Cu(II)-specific ligands present in surface sea waters [101]. Because of low concentrations, the exact nature of these ligands was unable to be established from LC–MS measurements, but possible structures posited included small peptide units and/or fragments from degraded siderophores.

Copper(II)-based IMAC has also been used to study ligands present in soil samples [102]. The retention behavior of a series of model ligands with variable Cu(II) affinities was examined, which showed that pyridine-type ligands and salicylhydroxamic acid were strongly retained on the Cu(II)–IDA matrix, and ligands containing carboxylic acid groups as the predominant ligand type were generally not retained.

1.4.6 Selecting a Viable Target

A multitude of octahedral heteroleptic metal–IDA or –NTA complexes exist that have been characterized in the solid state and in solution, in which the remaining sites in the coordination sphere are filled by a different tri- or bidentate ligand, respectively [103–105]. The non-IDA- or NTA-based ligands in these cases, or more complex compounds that contain these ligand types as substructures, represent candidates for isolation using IMAC, since the IMAC resin can be considered representative of the metal–IDA or –NTA component of the mixed ligand complex. Examples include solution structures characterized between [Fe(III)(NTA)$(OH_2)_2$] and acetohydroxamic acid [104], which accord with the successful capture of hydroxamic acid compounds, including DFOB and TSA on IDA-based IMAC resins [55, 82]. An X-ray crystal structure of the Fe(III)–NTA based heteroleptic complex with the fluoroquinoline antibiotic ciprofloxacin (R_1 = cyclopropane, R_2 = H, R_3 = piperazine, R_4 = H) (Fig. 1.10) showed that the complex [Fe(ciprofloxacin)(NTA)]·3.5H_2O featured coordination from ciprofloxacin through the keto and carboxylate oxygen atoms [106]. Ciprofloxacin and other fluoroquinoline-based analogues are synthetic products, rather than products of bacterial fermentation, which would find IMAC being a possible step for purification during chemical synthesis. The structural characterization of [Fe(ciprofloxacin)(NTA)]·3.5H_2O is consistent with the successful capture of fluoroquinoline-based antibiotic compounds using Fe(III)-based IMAC [97]. X-ray crystal structure data from heteroleptic complexes between Cu(II)–*N*-methyl-IDA and monodentate coordinated adenine [107] or bidentate acyclovir (also known as aciclovir) [108] support the use of IMAC for polynucleotide purification [109].

The X-ray crystal structure of the heteroleptic complex [Cu(IDA)(α-picolinamide)]·2H_2O [105] supports that Cu(II)–IDA based IMAC could be useful for the isolation of more complex natural products that feature α-picolinamide as a structural motif, including the vertilecanins, which were isolated and characterized from fermentations of the fungus *Verticillium lecanii*, and shown to have antibiotic properties [110]. The characterization of the heteroleptic complex [Ni(IDA)(DABT)(OH_2)] (DABT = 2,2′-diamino-4,4′-bi-1,3-thiazole) [111] supports that natural products containing the bithiazole motif would be candidates for IMAC-based purification. Examples of complex natural products with bithiazole groups include metabolites from the myxobacterium *Myxococcus fulvus*, including myxothiazole A [112], cystothiazoles [113], and melithiazoles [114], which have demonstrated various antimicrobial and cytotoxic effects [115]. Although selected members of this group of compounds can be produced from total synthesis [116, 117], the multi-step and complex syntheses give modest yields. As allowed by IMAC, a single-step isolation method direct from culture carries the advantages of both improved yield of the parent compound and the simultaneous capture of structural analogues for establishing chemical diversity. In addition to bithiazole-containing natural products, IMAC could be used for non-aromatic analogues, such as the siderophores

yersiniabactin and pyochelin, which contain a 4,2-linked thiazoline-thiazolidine system [118–120]. While IDA- or NTA-based heteroleptic complexes are the best guide for IMAC compatible ligands, other heteroleptic complexes can also be used to inform the selection process. As one example, the characterization of the heteroleptic Cu(II) complex formed with 2,2′-bipyridine and the natural product plumbagin [121], suggests that related naphthoquinone-based compounds present in *Plumbaginaceae* extracts used in traditional Chinese medicine [122], could be isolable using Cu(II)-based IMAC.

Another strategy to determine targets that would be amenable to isolation using IMAC is to consider metalloprotein inhibitors. The metal–ligand active site of a metalloprotein is most often coordinatively unsaturated, to allow for substrate docking and subsequent chemical transformation. The coordinatively unsaturated metal–IDA or –NTA resin can in effect be viewed as a surrogate of a metalloprotein active site. This opens up a powerful means to select for potential metalloprotein inhibitors from a complex mixture. This has proven successful in the use of Ni(II)-based IMAC for selecting TSA from *S. hygroscopicus* MST-AS5346 culture, as one of the most potent documented inhibitors of the Zn(II)-containing histone deacetylases [72, 82]. The bengamides, which are natural products isolated from sponge [123], have been shown to coordinate to the bimetallic Ni(II), Mn(II) or Co(II) active site of human or *Mycobacterium tuberculosis* methionine aminopeptidase via bridged coordination from the trihydroxy-substituted amide extension region [124, 125]. These types of compounds could potentially be isolable from the extract using Ni(II)-, Mn(II)- or Co(II)-based IMAC. The stoichiometry of the ternary immobilized bengamide–metal–IDA/NTA complex would likely be different from the bridged structure observed from the protein X-ray data, but the IMAC method remains compatible with the selection of this type of compound. Documentation of all natural products based inhibitors of metalloproteins is beyond the scope of this chapter, but these few examples serve to illustrate the use of protein X-ray crystallography data to guide the selection of targets isolable using IMAC.

In the absence of available data on metal–IDA or –NTA or other heteroleptic complexes, or guiding knowledge of the metalloprotein inhibitory activity of a compound, it is sufficient to simply explore the coordination chemistry of a potential target to assess its viability for selection using IMAC. Bacteria, fungi, plants, and sponges produce a multitude of chemically diverse natural products that serve as drugs themselves or as scaffolds for chemical modification or the design of synthetic analogues [126–130]. Candidate compounds that have a native metal binding ability, such as siderophores, or a metal ion binding requirement for activity, such as bleomycins, and other metalloantibiotics [131], are cases in point. The IMAC-based purification protocol can be guided by the types and configuration of donor atoms and the most appropriate IMAC-compatible metal ion, according to the HSAB theory [6] and other considerations of coordination chemistry. The aminoglycoside antibiotics, which include streptomycin, gentamycin, tobramycin, amikacin, neomyxin, and paromomycin, contain an extensive array of amino and hydroxyl groups, which would bind to a Cu(II)- or Fe(III)-based IMAC resin [99, 132]. We are currently using IMAC to purify other anticancer compounds from complex fermentation mixtures, including the aminoglycoside-based doxorubicin, which has a documented coordination chemistry with Cu(II) and Fe(III). Solution complexes of Cu(II) and the antibiotic lincomycin have been established using ^{1}H and ^{13}C NMR (nuclear magnetic resonance) spectroscopy [133], which supports that Cu(II)-based IMAC would be useful

in selecting for lincomycin and analogues from cultures of *Streptomyces lincolnensis*. The success of each of these examples will be dependent upon the water solubility of the target compound, since the IMAC procedure can generally tolerate only low levels of organic solvents, and is mostly incompatible with the use of coordinating solvents, such as methanol and dimethylformamide. Ultimately, it remains that experiment is the best guide to the efficacy of IMAC for the capture of non-protein based targets.

1.5 New Application 2: Multi-dimensional Immobilized Metal Ion Affinity Chromatography

Part of the driving force for developing IMAC for isolating non-protein based bacterial metabolites lies in the possibility of accessing more than one compound from a single culture. The ability to purify multiple components from a single mixture would increase production efficiency and streamline pharmaceutics processing. Two or more IMAC columns configured in series containing resins loaded with different metal ions could retain different classes of metabolites, as defined by differential metabolite–metal binding affinities. In our group, we have termed this IMAC mode, multi-dimensional IMAC (MD-IMAC). It could be predicted that each column would be enriched with a different class of metabolite, which would be recoverable upon disassembling the columns and eluting the bound components.

The original report on IMAC for the separation of serum proteins used an in-series configuration of Zn(II)- and Cu(II)-loaded IMAC resins [1]. Similar to the modest traction that IMAC itself garnered in its infancy (Fig. 1.4), the concept of using columns in series to gain additional resolving power essentially vanished from the literature, with only a few subsequent reports of this format, which were termed “tandem” IMAC [15] or “cascade” IMAC [134].

In our group, we are practising MD-IMAC for the resolution of more than one high-value clinical agent from a single culture. MD-IMAC has not previously been conducted to separate multiple bacterial secondary metabolites. Our preliminary experiments have focused upon the resolution of mixtures of standard solutions of DFOB and bleomycin. In single-dimensional IMAC, Ni(II)-based IMAC was effective for retaining a standard DFOB solution (Figs. 1.6 and 1.7) and Cu(II)-based IMAC was effective for retaining a standard bleomycin solution (Fig. 1.9). For the MD-IMAC format, significant resolution of these agents was achieved using Yb(III)-based IMAC for DFOB and Cu(II)-based IMAC for bleomycin (Fig. 1.11, panel on the left). The major difference between the results obtained in our work and the early results that used in-series columns for resolving serum proteins [1, 15], was that we observed a profound difference in the effect of the order of the columns. In the case where the column containing the Yb(III)-loaded resin was mounted above the column containing the Cu(II)-loaded resin, about 70% of the DFOB was retained on the Yb(III)-based resin, with about 30% DFOB, and the entire sample of bleomycin, retained on the Cu(II)-based resin. In the case where the column order was reversed, with the Cu(II)-loaded column mounted above the Yb(III)-loaded column, there was no resolution between DFOB and bleomycin, with both components retained on the upper Cu(II)-loaded resin (Fig. 1.11, panel on the right). This is an elegant

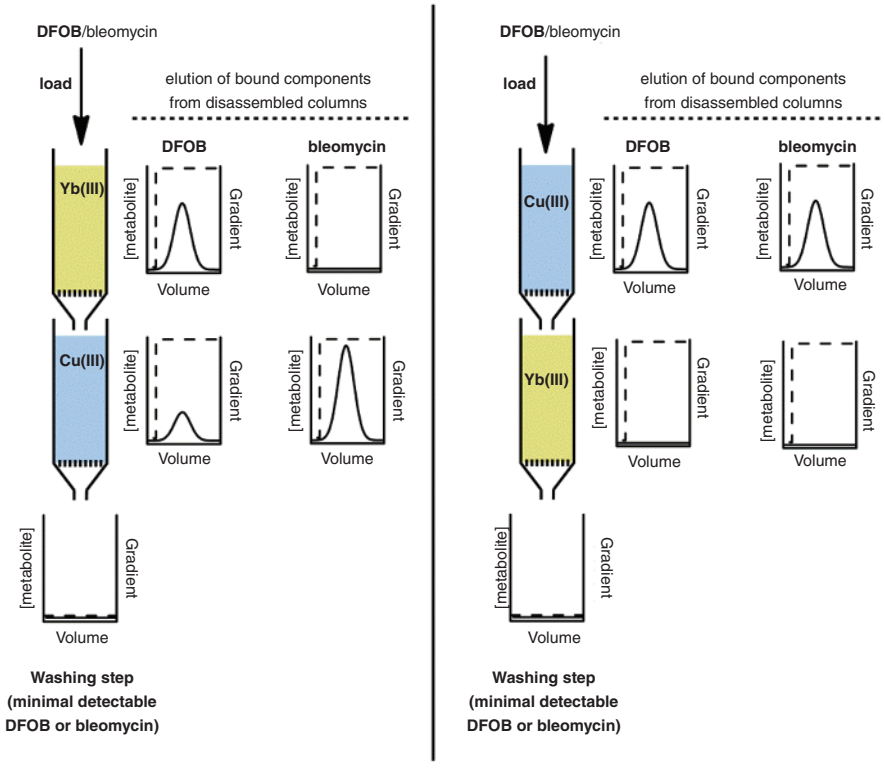

Figure 1.11 *Multi-dimensional immobilized metal ion affinity chromatography (MD-IMAC) for the separation of multiple bacterial secondary metabolites with differential metal ion affinities. In the MD-IMAC setup, two columns containing IMAC resins loaded with different metal ions are configured in series. After loading the mixture containing the analytes, the two columns are disassembled and the bound components are eluted from each column. The column order can affect the resolution: DFOB and bleomycin were well resolved using a Yb(III)-loaded resin mounted above a Cu(II)-loaded resin (left-hand side), but were not resolved using a Cu(II)-loaded resin mounted above a Yb(III)-loaded resin (right-hand side)*

example of the use of MD-IMAC and its underlying principle of separating non-protein based bacterial metabolites based upon differential metal ion affinities.

The successful partial resolution of DFOB and bleomycin was determined by the significant differential in binding affinities towards Yb(III). While DFOB has a significant affinity towards Yb(III) (log K 16.0), bleomycin, which has a combination of hard (*O*-based) and borderline (*N*-based) donor atoms in the metal-binding region (Fig. 1.9), has negligible affinity to the hard Yb(III) ion (log K not determined). In the case where the Cu(II) column was mounted above the Yb(III) column, the similarity in affinity constants of complexes between Cu(II) and DFOB (log K 14.1) or bleomycin (log K 12.6) resulted in both components binding to the Cu(II) column. In experiments that used in-series Cu(II)- and Fe(III)-IMAC formats to resolve serum proteins, there was no effect in the column order: the same protein profile was distributed across each column, independent of column order [15].

Multi-dimensional IMAC has significant potential for capturing multiple components from a single mixture. This could be used for pharmaceutics processing and also for targeted, analytical-scale separations of whole bacterial metabolomes, as discussed in the following section. In our work, we have used two in-series columns, but it would be possible to use additional columns, each loaded with a different metal ion. A hypothetical device that could advance MD-IMAC is shown in Fig. 1.12. In this device, multiple IMAC "cassettes" each containing a different metal ion are threaded in series in a Falcon tube-like housing. Following the binding step, which could be undertaken using gravity, pressure, or low centrifugal force, the cassettes would be disassembled and the components eluted from each individual cassette.

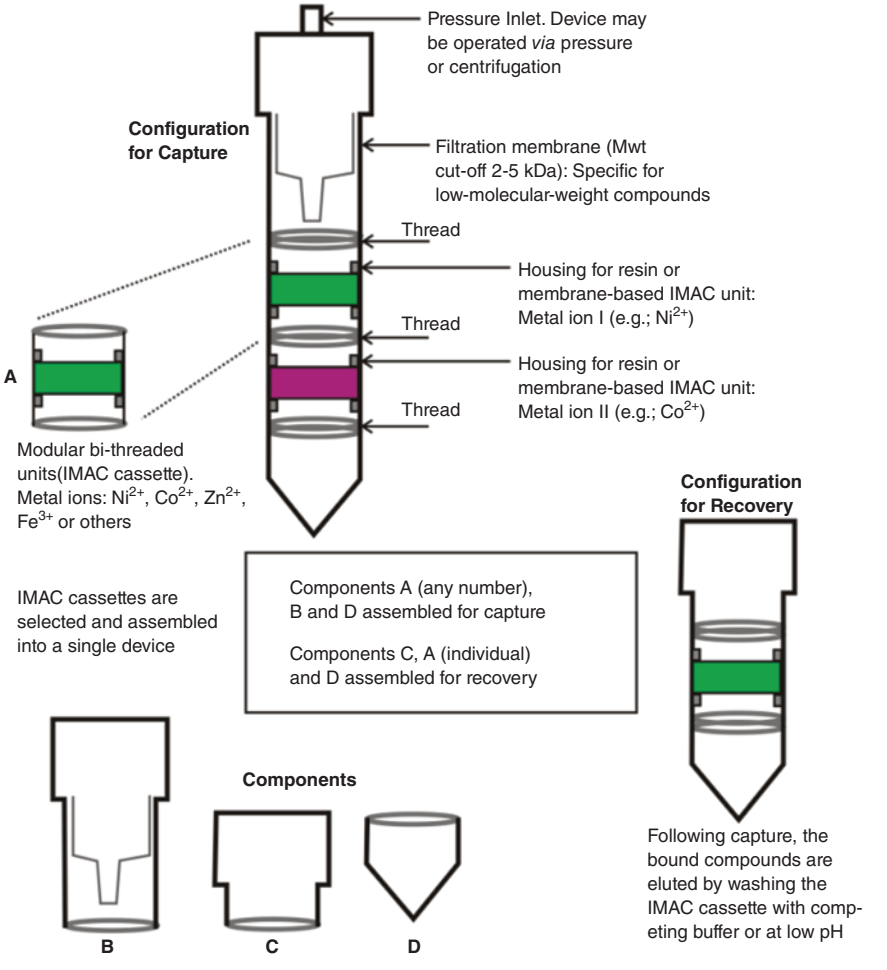

Figure 1.12 *A hypothetical device that could be used for multi-dimensional immobilized metal ion affinity chromatography (MD-IMAC) applications. This device shows individual IMAC "cassettes" threaded in series in a Falcon tube-like housing that could be subject to operation under low centrifugal force*

1.6 New Application 3: Metabolomics

Metabolomics is a recent addition to the "omics" family that describes the set of metabolites characteristic to a given species [135–138]. Each bacterial metabolome contains many hundreds of compounds and provides a rich resource for drug discovery [139, 140]. The bacterial metabolome also reports on the metabolic status of an organism, as modulated by the growth conditions local to the environment or host [141, 142]. While a given metabolome harbors a rich information content, its analysis is complicated by the sheer number of components, which are unable to be fully resolved for LC–MS analysis [142]. Separation technologies that reduce the complexity of a bacterial metabolome are needed to support metabolomics research across the health and environmental spheres.

IMAC offers the means to fractionate a bacterial metabolome into various pools of compounds with different metal ion affinities. By definition, the compounds that have no metal ion affinity will be removed from the whole metabolome. While this could be seen as a disadvantage, the concept does offer the potential to select for a significantly smaller population of compounds in a targeted fashion. The bacterial metabolome can be modulated *in situ* by external conditions, such as temperature and available nutrients, and also *in vitro* using precursor directed biosynthesis approaches, where non-native substrates are added to the growth medium for incorporation into native biosynthetic pathways to generate new compounds [143, 144]. IMAC would be well suited to profiling siderophore and bleomycin metabolomes, as well as the metabolomes of alternative IMAC-compatible compounds. As an example, precursor directed biosynthesis approaches have been used to generate new siderophore analogues of desferrioxamine E, pyochelin, and rhizoferrin [145–147]. More recently, the siderophore metabolome of *Shewanella putrefaciens* has been modulated [148] by inhibiting endogenous levels of the 1,4-diaminobutane substrate used in the biosynthesis of its native siderophore putrebactin [149]. Each of these siderophore metabolomes would be amenable to profiling using IMAC.

Our group is currently undertaking studies to map the siderophore metabolome of the marine bacterium *Salinispora tropica*. Marine bacteria, including *S. tropica*, and other *Actinomycetes*, are under scrutiny in natural products research, given the wealth of clinical compounds discovered from their terrestrial counterparts [150, 151]. *Salinispora tropica* has particular notoriety with regard to chemical diversity, since almost 10% of its genome codes for secondary metabolites [152]. These studies, to be published shortly, underpin the utility of IMAC for the selective capture of siderophores from culture. New erythromycin analogues prepared using a precursor-directed biosynthesis approach with an engineered strain of *Escherichia coli* [153] could be isolable using Fe(III)- or Cu(II)-based IMAC [97].

1.7 New Application 4: Coordinate-bond Dependent Solid-phase Organic Synthesis

In a recent development, the IMAC format has been extended beyond the affinity-based separation of non-protein based low molecular weight bacterial secondary metabolites. In this application, a bed of IMAC resin containing a bound bacterial metabolite was subject to solid-phase synthesis on this same resin bed, to furnish a derivative of the metabolite [154]. This method is efficient, since the same resin bed is used to both capture the molecule and for the downstream semi-synthetic chemistry. Conducting solid-phase organic synthesis

using a system where the primary molecule was bound to the IMAC resin via coordinate bonds carries all the advantages inherent to traditional solid-phase synthesis methods, in which the primary ligand is covalently bound to Merrifield resin, or Rink or Wang resins. The reaction was able to be driven to completion using an excess of reagents and these excess reagents and reaction byproducts were readily removed from the system via filtration. This method is distinct from other solid-phase organic synthesis methods by virtue of the immobilization of the primary ligand by multiple coordinate bonds rather than covalent bonds, and for this reason has been termed coordinate-bond dependent solid-phase organic synthesis (CBD-SPOS) [154].

In the first example of CBD-SPOS, a sample of DFOB was bound to Ni(II)-loaded IDA resin. At pH 9, DFOB is posited to bind to the IMAC resin via the hydroxamic acid functional groups with the pendant amine group remaining chemically reactive (Fig. 1.5), which was demonstrated by the orange color formed from reaction with 2,4,6,-trinitrobenzenesulfonic acid. Following DFOB binding, the water was exchanged for non- (or weakly) coordinating tetrahydrofuran (THF), which did not significantly compete with DFOB for the resin binding sites. Methanol and dimethylformamide were unsuitable solvents, since they acted as competitive ligands and displaced DFOB from the resin. The semi-synthetic target that was chosen was biotinylated DFOB. Biotin–DFOB was of interest, since it could be used as a molecular probe against the cognate cell proteome of the native DFOB producing bacterium *S. pilosus*. Reaction between DFOB-bound Ni(II)-loaded IDA resin and *N*-hydroxysuccinimide–biotin in THF at 40 °C overnight yielded biotin–DFOB, which remained bound to the resin (Fig. 1.13). Less than 1% of the DFOB was leached from the resin during this procedure. The resin was washed exhaustively with THF, which leached a minimal amount of product (<1%) from the resin.

The CBD-SPOS product was eluted from the resin with water at pH 6.0. This pH value was sufficiently acidic to displace the DFOB-based products from the resin (pH 6 < pK_a hydroxamic acid (pK_a 9.0)), but was not so acidic as to dissociate the immobilized Ni(II)–IDA coordination complex (pH 6 > pK_a IDA (pK_a 2.5)), which resulted in the liberation of biotin–DFOB as a metal-free adduct. The yield of biotin–DFOB was 76% and the product was significantly purer than the equivalent product prepared using traditional solution phase chemistry (Fig. 1.14). The veracity of the method depended upon the strength of the multiple coordinate bonds between DFOB and the immobilized Ni(II)–IDA chelate being functionally equivalent to a covalent bond, as used in traditional SPOS methods. Methods that use metabolites as molecular probes are keenly sought in metabolomics/proteomics applications [155–158], and CBD-SPOS delivers a new methodology to access these probes. We are currently using CBD-SPOS to prepare chemical probes of alternative amine-functionalized siderophores, including pyoverdine type II, which is produced by pathogenic *Pseudomonas aeruginosa* [31, 159, 160], and other siderophores native to bacterial pathogens, including ornibactin C-4 from *Burkholderia cepacia* [161], and exochelin MN from *Mycobacterium neoaurum* [162, 163].

1.8 Green Chemistry Technology

One of the major advantages of IMAC for metabolite capture is that the technique is water compatible. In experiments aimed to isolate DFOB from *S. pilosus* culture, the aqueous supernatant was adjusted to pH 9.0, as the only pre-treatment step before being loaded onto

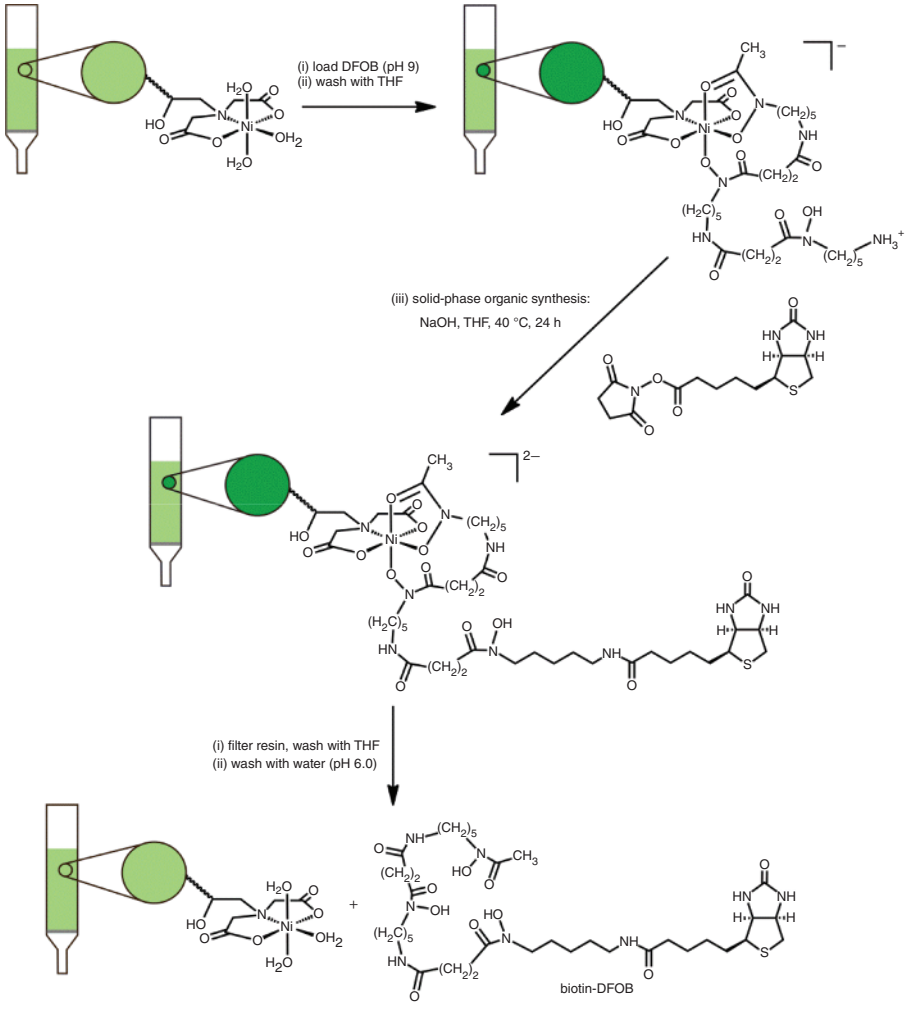

Figure 1.13 *Use of Ni(II)-loaded IMAC resin for the preparation of metal-specific probes and other semi-synthetic derivatives via coordinate-bond dependent solid-phase organic synthesis (CBD-SPOS). In CBD-SPOS, a metabolite with a chemically reactive group (e.g., amine) that is not involved in binding to the IMAC resin can be directly subjected to solid-phase chemical conversion on the same IMAC resin bed. This method carries all the advantages inherent to traditional solid-phase synthesis and has been used successfully to prepare biotin–DFOB under mild conditions. Adapted with permission from[154] © 2012 Royal Society of Chemistry*

an Ni(II)–IDA resin [55]. The retention of this compound, and of TSA in subsequent work [82], was undertaken entirely in the absence of organic solvents, and highlights the tenets of Green Chemistry inherent to IMAC processing. In other applications, components present in the bacteriological medium, including amino acids, peptides, and vitamins, which could compete for the metal-binding sites, can be removed using XAD-2 chromatography prior to IMAC processing [94]. This will improve the performance of the metal ion affinity step,

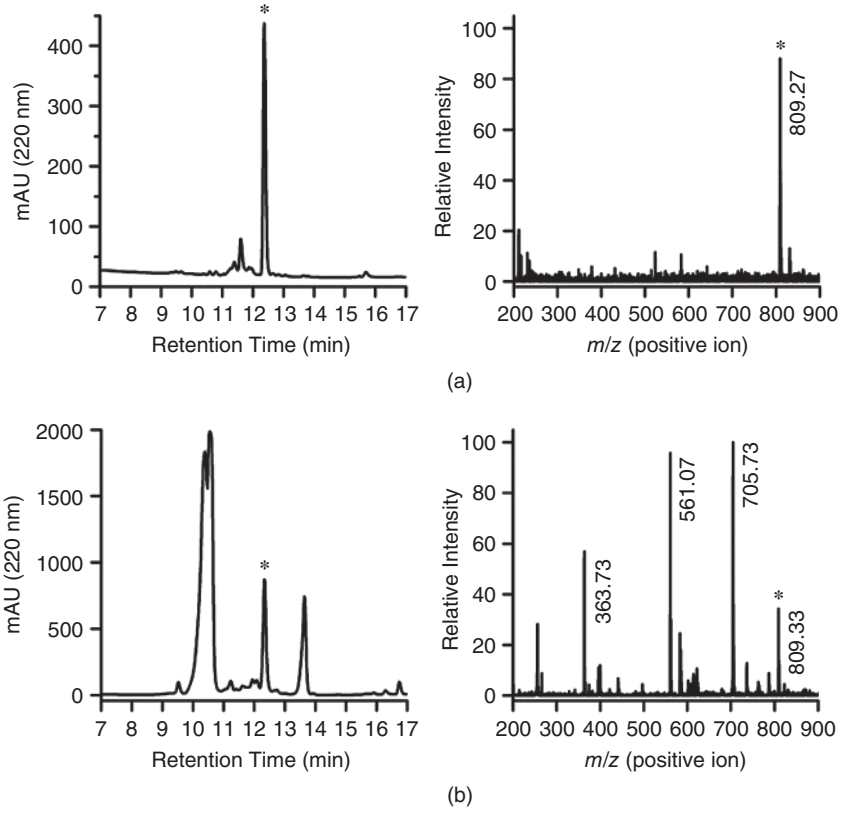

Figure 1.14 *Biotin-DFOB ($[M+Na^+]^+$, m/z_{calc} 809.42, *) was prepared in 76% yield and high purity using coordinate-bond dependent solid-phase organic synthesis (CBD-SPOS) (a), compared with conventional solution methods (b). Adapted with permission from [154] © 2012 Royal Society of Chemistry*

but does so at the expense of efficiency with the additional chromatographic step. One of the major goals in Green Chemistry is to reduce the use of organic solvents [164–166]. In pharmaceutics production, the extraction of clinical agents from fermentation mixtures may rely on the use of large volumes of organic solvents. This is the case for the current production of bleomycin [167] and also for DFOB, with 75% of the total production costs of the latter agent due to purification. Scaling IMAC processing to industrial scale could enable a significant reduction in the use of organic solvents in pharmaceutics processing. Further, the water compatibility of IMAC is particularly useful in natural products chemistry, since separating the polar components from an extract is generally more difficult than resolving the organic soluble components.

1.9 Conclusion

Based on the recent research from our laboratory and from other groups described in this chapter, it is evident that the applications of IMAC have not yet been exhausted. This

technique, with regard to the isolation of single or multiple non-protein based low molecular weight bacterial metabolites direct from complex fermentation mixtures, has a rich future in sustainable pharmaceutics processing. The use of in-series columns to obtain resins that are enriched with different classes of metabolites can increase purification efficiency, which is often the major cost in producing agents for clinical use. This technique has utility for mapping the metabolomes of selected classes of non-protein based bacterial metabolites with native metal binding affinity, including, but not limited to, siderophores and bleomycins. This has implications for discovering new drugs and for metabolomics to gain an understanding of how the local environment of a given bacterial species modulates the type and/or relative concentrations of these metabolites. This provides experimental data to complement systems biology approaches to drug discovery and environmental research.

The types of IMAC formats developed by the biotechnology sector aimed at automating recombinant protein purification are ever expanding. These newer IMAC-based formats, which include 96-well plates, membranes, magnetic beads, and quantum dots [168] are all transferable to the applications described in this chapter, relating to non-protein based low molecular weight metal binding compounds. These formats herald a bright future for the use of IMAC in natural products discovery and in pharmaceutics processing.

One of the major advantages of IMAC is its water compatibility. In this age of Green Chemistry, there is a strong drive to reduce the use of large volumes of organic solvents for extracting new chemical entities from natural sources: IMAC meets this remit. The authors look forward to continuing their contributions to expanding the scope of IMAC and envisage a future where this easy-to-use method is more fully integrated into chemical biology research platforms.

Acknowledgments

Ms Douha Lozi is acknowledged for contributions to the early phase of this work. The work has been supported by an Australian Postgraduate Award (J.G.) and with funding from The University of Sydney (Bridging Support Grants (R.C.), University Postgraduate Awards (N.E., T.L.)) and the National Health and Medical Research Council of Australia (R.C.).

References

1. Porath, J., Carlsson, J., Olsson, I., Belfrage, G. (1975) Metal chelate affinity chromatography, a new approach to protein fractionation. Nature, 258: 598–599.
2. Andersson, L., Porath, J. (1986) Isolation of phosphoproteins by immobilized metal (Fe^{3+}) affinity chromatography. Anal. Biochem., 154: 250–254.
3. Nühse, T. S., Stensballe, A., Jensen, O. N., Peck, S. C. (2003) Large-scale analysis of *in vivo* phosphorylated membrane proteins by immobilized metal ion affinity chromatography and mass spectrometry. Mol. Cell. Proteomics, 2: 1234–1243.
4. Imam-Sghiouar, N., Joubert-Caron, R., Caron, M. (2005) Application of metal-chelate affinity chromatography to the study of the phosphoproteome. Amino Acids, 28: 105–109.

5. Österberg, R. (1957) Metal and hydrogen-ion binding properties of *O*-phosphoserine. Nature, 179: 476–477.
6. Pearson, R. G. (1963) Hard and soft acids and bases. J. Am. Chem. Soc., 85: 3533–3539.
7. Jiang, W., Graham, B., Spiccia, L., Hearn, M. T. W. (1998) Protein selectivity with immobilized metal ion-tacn sorbents: chromatographic studies with human serum proteins and several other globular proteins. Anal. Biochem., 255: 47–58.
8. Zachariou, M., Hearn, M. T. W. (2000) Adsorption and selectivity characteristics of several human serum proteins with immobilized hard Lewis metal ion-chelate adsorbents. J. Chromatogr. A, 890: 95–116.
9. Chaouk, H., Hearn, M. T. W. (1999) New ligand, *N*-(2-pyridylmethyl)aminoacetate, for use in the immobilized metal ion affinity chromatographic separation of proteins. J. Chromatogr. A, 852: 105–115.
10. Cheung, R. C. F., Wong, J. H., Ng, T. B. (2012) Immobilized metal ion affinity chromatography: a review on its applications. Appl. Microbiol. Biotechnol., 96: 1411–1420.
11. Block, H., Maertens, B., Spriestersbach, A., Brinker, N., Kubicek, J., Fabis, R., Labahn, J., Schäfer, F. (2009) Immobilized-metal affinity chromatography: a review. Methods Enzymol., 463: 439–473.
12. Gutierrez, R., Martin del Valle, E. M., Galan, M. A. (2007) Immobilized metal-ion affinity chromatography: Status and trends. Sep. Purif. Rev., 36: 71–111.
13. Chaga, G. S. (2001) Twenty-five years of immobilized metal ion affinity chromatography: past, present and future. J. Biochem. Biophys. Methods, 49: 313–334.
14. Gaberc-Porekar, V., Menart, V. (2001) Perspectives of immobilized-metal affinity chromatography. J. Biochem. Biophys. Methods, 49: 335–360.
15. Porath, J., Olin, B. (1983) Immobilized metal ion affinity adsoption and immobilized metal ion affnity chromatography of biomaterials. Serum protein affinities for gel-immobilized iron and nickel ions. Biochemistry, 22: 1621–1630.
16. Priestman, D. A., Butterworth, J. (1985) Prolinase and non-specific dipeptidase of human kidney. Biochem. J., 231: 689–694.
17. Hochuli, E., Bannwarth, W., Döbeli, H., Gentz, R., Stüber, D. (1988) Genetic approach to facilitate purification of recombinant proteins with a novel metal chelate adsorbent. Bio/Technology, 6: 1321–1325.
18. Bucar, F., Wube, A., Schmid, M. (2013) Natural product isolation - how to get from biological material to pure compounds. Nat. Prod. Rep., 30: 525–545.
19. Budzikiewicz, H. (2010) Microbial siderophores, in: Kinghorn, A. D., Falk, H. and Kobayashi, J. (eds) *Progress in the Chemistry of Organic Natural Products*, pp. 1–75 (New York, Springer-Verlag).
20. Hider, R. C., Kong, X. (2010) Chemistry and biology of siderophores. Nat. Prod. Rep., 27: 637–657.
21. Neilands, J. B. (1995) Siderophores: structure and function of microbial iron transport compounds. J. Biol. Chem., 270: 26723–26726.
22. Raymond, K. N., Dertz, E. A. (2004) Biochemical and physical properties of siderophores, in: Crosa, J. H., Mey, A. R. and Payne, S. M. (eds) *Iron Transport in Bacteria*, pp. 3–17 (Washington, DC, ASM Press).

23. Crumbliss, A. L., Harrington, J. M. (2009) Iron sequestration by small molecules: thermodynamic and kinetic studies of natural siderophores and synthetic model complexes. Adv. Inorg. Chem., 61: 179–250.
24. Butler, A., Theisen, R. M. (2010) Iron(III)-siderophore coordination chemistry: Reactivity of marine siderophores. Coord. Chem. Rev., 254: 288–296.
25. Boukhalfa, H., Crumbliss, A. L. (2002) Chemical aspects of siderophore mediated iron transport. BioMetals, 15: 325–339.
26. Miethke, M., Marahiel, M. A. (2007) Siderophore-based iron acquisition and pathogen control. Microbiol. Mol. Biol. Rev., 71: 413–451.
27. Miethke, M. (2013) Molecular strategies of microbial iron assimilation: from high-affinity complexes to cofactor assembly systems. Metallomics, 5: 15–28.
28. Codd, R. (2008) Traversing the coordination chemistry and chemical biology of hydroxamic acids. Coord. Chem. Rev., 252: 1387–1408.
29. Scott, L. E., Orvig, C. (2009) Medicinal inorganic chemistry approaches to passivation and removal of aberrant metal ions in disease. Chem. Rev., 109: 4885–4910.
30. Marmion, C. J., Griffith, D., Nolan, K. B. (2004) Hydroxamic acids. An intriguing family of enzyme inhibitors and biomedical ligands. Eur. J. Inorg. Chem.: 3003–3016.
31. Schalk, I. J., Hannauer, M., Braud, A. (2011) New roles for bacterial siderophores in metal transport and tolerance. Environ. Microbiol., 13: 2844–2854.
32. Telpoukhovskaia, M. A., Orvig, C. (2013) Werner coordination chemistry and neurodegeneration. Chem. Soc. Rev., 42: 1836–1846.
33. Casentini, B., Pettine, M. (2010) Effects of desferrioxamine-B on the release of arsenic from volcanic rocks. Appl. Geochem., 25: 1688–1698.
34. Duckworth, O. W., Bargar, J. R., Sposito, G. (2009) Quantitative structure-activity relationships for aqueous metal-siderophore complexes. Environ. Sci. Technol., 43: 343–349.
35. Liddell, J. R., Obando, D., Liu, J., Ganio, G., Volitakis, I., Mok, S. S., Crouch, P. J., White, A. R., Codd, R. (2013) Lipophilic adamantyl- or deferasirox-based conjugates of desferrioxamine B have enhanced neuroprotective capacity: implications for Parkinson disease. Free Radic. Biol. Med., 60: 147–156.
36. Gez, S., Luxenhofer, R., Levina, A., Codd, R., Lay, P. A. (2005) Chromium(V) complexes of hydroxamic acids: Formation, structures, and reactivities. Inorg. Chem., 44: 2934–2943.
37. Pakchung, A. A. H., Soe, C. Z., Codd, R. (2008) Studies of iron-uptake mechanisms in two bacterial species of the *Shewanella* genus adapted to middle-range (*Shewanella putrefaciens*) or Antarctic (*Shewanella gelidimarina*) temperatures. Chem. Biodivers., 5: 2113–2123.
38. Pakchung, A. A. H., Soe, C. Z., Lifa, T., Codd, R. (2011) Complexes formed in solution between vanadium(IV)/(V) and the cyclic dihydroxamic acid putrebactin or linear suberodihydroxamic acid. Inorg. Chem., 50: 5978–5989.
39. Drechsel, H., Winkelmann, G. (1997) Iron Chelation and Siderophores, in: Winkelmann, G. and Carrano, C. J. (eds) *Transition Metals in Microbial Metabolism*, pp. 1–49 (Amsterdam, Harwood Academic).
40. Bernhardt, P. V. (2007) Coordination chemistry and biology of chelators for the treatment of iron overload disorders. Dalton Trans., 3214–3220.

41. Liu, J., Obando, D., Schipanski, L. G., Groebler, L. K., Witting, P. K., Kalinowski, D. S., Richardson, D. R., Codd, R. (2010) Conjugates of desferrioxamine B (DFOB) with derivatives of adamantane or with orally available chelators as potential agents for treating iron overload. J. Med. Chem., 53: 1370–1382.
42. Kalinowski, D. S., Richardson, D. R. (2005) The evolution of iron chelators for the treatment of iron overload disease and cancer. Pharmacol. Rev., 57: 547–583.
43. Martell, A. E., Smith, R. M. (1974) Critical Stability Constants. Vol. 1. (New York, Plenum Press).
44. Martell, A. E., Smith, R. M. (1977) Critical Stability Constants. Vol. 3. (New York, Plenum Press).
45. Sugiura, Y., Ishizu, K., Miyoshi, K. (1979) Studies of metallobleomycins by electronic spectroscopy, electron spin resonance spectroscopy, and potentiometric titration. J. Antibiot., 32: 453–461.
46. Khan, M. A., Lelie, D., Cornelis, P., Mergeay, M. (1994) Purification and characterization of "alcaligin E", a hydroxamate-type siderophore produced by *Alcaligenes eutrophus* CH 34, Conference Proceedings of the *Plant Pathogenic Bacteria: 8th International Conference*, Versailles, France, 1992, pp. 591–597.
47. Gilis, A., Khan, M. A., Cornelis, P., Meyer, J.-M., Mergeay, M., van der Lelie, D. (1996) Siderophore-mediated iron uptake in *Alcaligenes eutrophus* CH34 and identificatoin of *ale*B encoding the ferric iron-alcaligin E receptor. J. Bacteriol., 178: 5499–5507.
48. Münzinger, M., Taraz, K., Budzikiewicz, H. (1999) Staphyloferrin B, a citrate siderophore of *Ralstonia eutropha*. Z. Naturforsch. C., 54: 867–875.
49. Harris, W. R., Carrano, C. J., Raymond, K. N. (1979) Coordination chemistry of microbial iron transport compounds. 16. Isolation, characterization and formation constants of ferric aerobactin. J. Am. Chem. Soc., 101: 2722–2727.
50. Stemmler, A. J., Kampf, J. W., Kirk, M. L., Pecoraro, V. L. (1995) A model for the inhibition of urease by hydroxamates. J. Am. Chem. Soc., 117: 6368–6369.
51. Benini, S., Rypniewski, W. R., Wilson, K. S., Miletti, S., Ciurli, S., Mangani, S. (2000) The complex of *Bacillus pasteurii* urease with acetohydroxamate anion from X-ray data at 1.55 Å resolution. J. Biol. Inorg. Chem., 5: 110–118.
52. Gaynor, D., Starikova, Z. A., Ostrovsky, S., Haase, W., Nolan, K. B. (2002) Synthesis and structure of a heptanuclear nickel(II) complex uniquely exhibiting four distinct binding modes, two of which are novel, for a hydroxamate ligand. Chem. Commun., 506–507.
53. Brown, D. A., Geraty, R., Glennon, J. D., Choileain, N. N. (1986) Design of metal chelates with biological activity. 5. Complexation behavior of dihydroxamic acids with metal ions. Inorg. Chem., 25: 3792–3796.
54. Fazary, A. E. (2005) Thermodynamic studies on the protonation equilibria of some hydroxamic acids in $NaNO_3$ solutions in water and in mixtures of water and dioxane. J. Chem. Eng. Data, 50: 888–895.
55. Braich, N., Codd, R. (2008) Immobilized metal affinity chromatography for the capture of hydroxamate-containing siderophores and other Fe(III)-binding metabolites from bacterial culture supernatants. Analyst, 133: 877–880.

56. Keller-Schierlein, W., Mertens, P., Prelog, V., Wasler, A. (1965) Metabolic products of microorganisms. XLIX. Ferrioxamines A1, A2, and D2. Helv. Chim. Acta, 48: 710–723.
57. De Voss, J. J., Rutter, K., Schroeder, B. G., Su, H., Zhu, Y., Barry, C. E. I. (2000) The salicylate-derived mycobactin siderophores of *Mycobacterium tuberculosis* are essential for growth in macrophages. Proc. Natl. Acad. Sci. USA, 97: 1252–1257.
58. Zane, H. K., Butler, A. (2013) Isolation, structure elucidation, and iron-binding properties of lystabactins, siderophores isolated from a marine *Pseudoaltermonas* sp. J. Nat. Prod., 76: 648–654.
59. Rehder, D. (1999) The coordination chemistry of vanadium as related to its biological functions. Coord. Chem. Rev., 182: 297–322.
60. Butler, A., Parsons, S. M., Yamagata, S. K., de la Rosa, R. I. (1989) Reactivation of vanadate-inhibited enzymes with desferrioxamine B, a vanadium(V) chelator. Inorg. Chim. Acta, 163: 1–3.
61. Bell, J. H., Pratt, R. F. (2002) Mechanism of inhibition of the β-lactamase of *Enterobacter cloacae* P99 by 1:1 complexes of vanadate with hydroxamic acids. Biochemistry, 41: 4329–4338.
62. Goldwaser, I., Li, J., Gershonov, E., Armoni, M., Karnieli, E., Fridkin, M., Shechter, Y. (1999) L-Glutamic acid γ-monohydroxamate. A potentiator of vanadium-evoked glucose metabolism in vitro and in vivo. J. Biol. Chem., 274: 26617–26624.
63. Haratake, M., Fukunaga, M., Ono, M., Nakayama, M. (2005) Synthesis of vanadium(IV,V) hydroxamic acid complexes and *in vivo* assessment of their insulin-like activity. J. Biol. Inorg. Chem., 10: 250–258.
64. Luterotti, S., Grdinic, V. (1986) Spectrophotometric determination of vanadium(V) with desferrioxamine B. Analyst, 111: 1163–1165.
65. Minucci, S., Pelicci, P. G. (2006) Histone deacetylase inhibitors and the promise of epigenetic (and more) treatments for cancer. Nat. Rev. Cancer, 6: 38–51.
66. Bolden, J. E., Peart, M. J., Johnstone, R. W. (2006) Anticancer activities of histone deacetylase inhibitors. Nat. Rev. Drug Discov., 5: 769–784.
67. Liu, T., Kuljaca, S., Tee, A., Marshall, G. M. (2006) Histone deacetylase inhibitors: multifunctional anticancer agents. Cancer Treat. Rev., 32: 157–165.
68. Bertrand, P. (2010) Inside HDAC with HDAC inhibitors. Eur. J. Med. Chem., 45: 2095–2116.
69. Marks, P. A., Breslow, R. (2007) Dimethylsulfoxide to vorinostat: Development of this histone deacetylase inhibitor as an anticancer drug. Nat. Biotechnol., 25: 84–90.
70. Codd, R., Braich, N., Liu, J., Soe, C. Z., Pakchung, A. A. H. (2009) Zn(II)-dependent histone deacetylase inhibitors: suberoylanilide hydroxamic acid and trichostatin A. Int. J. Biochem. Cell Biol., 41: 736–739.
71. Liao, V., Liu, T., Codd, R. (2012) Amide-based derivatives of β-alanine hydroxamic acid as histone deacetylases inhibitors: Attenuation of potency through resonance effects. Bioorg. Med. Chem. Lett., 22: 6200–6204.
72. Bieliauskas, A. V., Pflum, M. K. H. (2008) Isoform-selective histone deacetylase inhibitors. Chem. Soc. Rev., 37: 1402–1413.
73. Tsuji, N., Kobayashi, M., Nagashima, K., Wakisaka, Y., Koizumi, K. (1976) A new antifungal antibiotic, trichostatin. J. Antibiot., 29: 1–6.

74. Woo, S. H., Frechette, S., Khalil, E. A., Bouchain, G., Vaisburg, A., Bernstein, N., Moradei, O., Leit, S., Allan, M., Fournel, M., Trachy-Bourget, M.-C., Li, Z., Besterman, J. M., Delorme, D. (2002) Structurally simple trichostatin A-like straight chain hydroxamates as potent histone deacetylase inhibitors. J. Med. Chem., 45: 2877–2885.
75. Anzellotti, A. I., Farrell, N. P. (2008) Zinc metalloproteins as medicinal targets. Chem. Soc. Rev., 37: 1629–1651.
76. Puerta, D. T., Cohen, S. M. (2004) A bioinorganic perspective on matrix metalloproteinase inhibition. Curr. Top. Med. Chem., 4: 1551–1573.
77. Whittaker, M., Floyd, C. D., Brown, P., Gearing, A. J. H. (1999) Design and therapeutic application of matrix metalloproteinase inhibitors. Chem. Rev., 99: 2735–2776.
78. Hu, J., Van den Steen, P. E., Sang, Q.-X. A., Opdenakker, G. (2007) Matrix metalloproteinase inhibitors as therapy for inflammatory and vascular diseases. Nat. Rev. Drug. Discov., 6: 480–498.
79. Finnin, M. S., Donigian, J. R., Cohen, A., Richon, V. M., Rifkind, R. A., Marks, P. A., Breslow, R., Pavletich, N. P. (1999) Structures of a histone deacetylase homologue bound to the TSA and SAHA inhibitors. Nature, 401: 188–193.
80. Griffith, D. M., Szöcs, B., Keogh, T., Suponitsky, K. Y., Farkas, E., Buglyó, P., Marmion, C. J. (2011) Suberoylanilide hydroxamic acid, a potent histone deacetylase inhibitor; its X-ray crystal structure and solid state and solution studies of its Zn(II), Ni(II), Cu(II) and Fe(III) complexes. J. Inorg. Biochem., 105: 763–769.
81. Zhang, S., Duan, W., Wang, W. (2006) Efficient, enantioselective organocatalytic synthesis of trichostatin A. Adv. Synth. Catal., 348: 1228–1234.
82. Ejje, N., Lacey, E., Codd, R. (2012) Analytical-scale purification of trichostatin A from bacterial culture in a single step and with high selectivity using immobilised metal affinity chromatography. RSC Adv., 2: 333–337.
83. Umezawa, H., Takita, T. (1980) The bleomycins: Antitumor copper-binding antibiotics. Struct. Bond., 40: 73–99.
84. Chen, J., Stubbe, J. (2005) Bleomycins: Towards better therapeutics. Nat. Rev. Cancer, 5: 102–112.
85. Galm, U., Hager, M. H., Van Lanen, S. G., Ju, J., Thorson, J. S., Shen, B. (2005) Antitumor antibiotics: Bleomycin, enediyenes, and mitomycin. Chem. Rev., 105: 739–758.
86. Einhorn, L. H. (2002) Curing metastatic testicular cancer. Proc. Natl. Acad. Sci. USA, 99: 4592–4595.
87. Aoyagi, Y., Katano, K., Suguna, H., Primeau, J., Chang, L.-H., Hecht, S. M. (1982) Total synthesis of bleomycin. J. Am. Chem. Soc., 104: 5537–5538.
88. Sugiyama, M., Kumagai, T., Hayashida, M., Maruyama, M. (2002) The 1.6-Å crystal structure of the copper(II)-bound bleomycin complexed with the bleomycin-binding protein from bleomycin-producing Streptomycin verticillus. J. Biol. Chem., 277: 2311–2320.
89. Iitaka, Y., Nakamura, H., Nakatani, T., Muraoka, Y., Fujii, A., Takita, T., Umezawa, H. (1978) Chemistry of bleomycin. XX The X-ray structure determination of P-3A Cu(II)-complex, a biosynthetic intermediate of bleomycin. J. Antibiot., 31: 1070–1072.

90. Decker, A., Chow, M. S., Kemsley, J. N., Lehnert, N., Solomon, E. I. (2006) Direct hydrogen-atom abstraction by activated bleomycin: An experimental and computational study. J. Am. Chem. Soc., 128: 4719–4733.
91. Sam, J. W., Tang, X.-J., Peisach, J. (1994) Electrospray mass spectrometry of iron bleomycin: Demonstration that activated bleomycin is a ferric peroxide complex. J. Am. Chem. Soc., 116: 5250–5256.
92. Burger, R. M., Peisach, J., Horwitz, S. B. (1981) Activated bleomycin. A transient complex of drug, iron, and oxygen that degrades DNA. J. Biol. Chem., 256: 11636–11644.
93. Westre, T. E., Loeb, K. E., Zaleski, J. M., Hedman, B., Hodgson, K. O., Solomon, E. I. (1995) Determination of the geometric and electronic structure of activated bleomycin using X-ray absorption spectroscopy. J. Am. Chem. Soc., 117: 1309–1313.
94. Gu, J., Codd, R. (2012) Copper(II)-based metal affinity chromatography for the isolation of the anticancer agent bleomycin from *Streptomyces verticillus* culture. J. Inorg. Biochem., 115: 198–203.
95. Bewley, M. C., Jeffrey, P. D., Patchett, M. L., Kanyo, Z. F., Baker, E. N. (1999) Crystal structure of *Bacillus caldovelox* arginase in complex with substrate and inhibitors reveal new insights into activation, inhibition and catalysis in the arginase superfamily. Structure, 7: 435–448.
96. Ahn, H.-J., Kim, K. H., Lee, J. K., Ha, J.-Y., Lee, H. H., Kim, D., Yoon, H.-J., Kwon, A.-R., Suh, S. W. (2004) Crystal structure of agmatinase reveals structural conservation and inhibition mechanism of the ureohydrolase superfamily. J. Biol. Chem., 279: 50505–50513.
97. Takeda, N., Matsuoka, T., Gotoh, M. (2010) Potentiality of IMAC as sample pretreatment tool in food analysis for veterinary drugs. Chromatographica, 72: 127–131.
98. Drechsel, H., Fiallo, M., Garnier-Suillerot, A., Matzanke, B. F., Schünemann, V. (2001) Spectroscopic studies on iron complexes of different anthracyclines in aprotic solvent systems. Inorg. Chem., 40: 5324–5333.
99. Gokhale, N., Patwardhan, A., Cowan, J. A. (2007) Metalloaminoglycosides: Chemistry and biological relevance, in: Arya, D. P. (ed.) *Aminoglycoside Antibiotics: From Chemical Biology to Drug Discovery*, pp. 235-254 (Hoboken, NJ, Wiley-Interscience).
100. Chen, Z.-F., Tang, Y.-Z., Liang, H., Zhong, X.-X., Li, Y. (2006) Cobalt(II)-promoted hydrolysis of cephalexin: crystal structure of the cephalosporate-cobalt(II) complex. Inorg. Chem. Commun., 9: 322–325.
101. Ross, A. R. S., Ikonomou, M. G., Orians, K. J. (2003) Characterization of copper-complexing ligands in seawater using immobilized copper(II)-ion affinity chromatography and electrospray ionization mass spectrometry. Mar. Chem., 83: 47–58.
102. Paunovic, I., Schulin, R., Nowack, B. (2005) Evaluation of immobilized metal-ion affinity chromatography for the fractionation of natural Cu complexing ligands. J. Chromatogr., Sect. A., 1100: 176–184.
103. Kruppa, M., König, B. (2006) Reversible coordinative bonds in molecular recognition. Chem. Rev., 106: 3520–3560.

104. Gabričević, M., Crumbliss, A. L. (2003) Kinetics and mechanism of iron(III)-nitrilotriacetate complex reactions with phosphate and acetohydroxamic acid. Inorg. Chem., 42: 4098–4101.
105. Bugella-Altamirano, E., González-Pérez, J. M., Choquesillo-Lazarte, D., Niclós-Gutiérrez, J., Castiñeiras-Campos, A. (2000) Structural relationships obtained from the coordination of α-picolinamide to the (iminodiacetato)copper(II) chleate: synthesis, crystal structure, and properties of (α-picolinamide)(iminodiacetato) copper(II) dihydrate. Z. Anorg. Allg. Chem., 626: 930–936.
106. Wallis, S. C., Gahan, L. R., Charles, B. G., Hambley, T. W. (1995) Synthesis and X-ray structural characterisation of an iron(III) complex of the fluoroquinoline antimicrobial ciprofloxacin, [Fe(CIP)(NTA)]3.5H_2O (NTA = nitrilotriacetato). Polyhedron, 14: 2835–2840.
107. Bugella-Altamirano, E., Choquesillo-Lazarte, D., González-Pérez, J. M., Sánchez-Moreno, M. J., Marín-Sánchez, R., Martín-Ramoa, J. D., Covelo, B., Carballo, R., Castiñeiras, A., Niclós-Gutiérrez, J. (2002) Three new modes of adenine-copper(II) coordination: interligand interactions controlling the selective N3-, N7- and bridging μ-N3,N7-metal-bonding of adenine to different N-substituted iminodiacetato-copper(II) chelates. Inorg. Chim. Acta, 339: 160–170.
108. del Pilar Brandi-Blanco, M., Choquesillo-Lazarte, D., Domínguez-Martín, A., González-Pérez, J. M., Castiñeiras, A., Niclós-Gutiérrez, J. (2011) Metal ion binding patterns of acyclovir: Molecular recognition between this antiviral agent and copper(II) chelates with iminodiacetate or glycylglycinate. J. Inorg. Biochem., 105: 616–623.
109. Kanakaraj, I., Jewell, D. L., Murphy, J. C., Fox, G. E., Wilson, R. C. (2011) Removal of PCR error products and unincorporated primers by metal-chelate affinity chromatography. PLoS ONE, 6: e14512. doi:10.1371/journal.pone.0014512.
110. Soman, A. G., Gloer, J. B., Angawi, R. F., Wicklow, D. T., Dowd, P. F. (2001) Vertilecanins: new phenopicolinic acid analogues from *Verticillium lecanii*. J. Nat. Prod., 64: 189–192.
111. Liu, J.-G., Xu, D.-J. (2005) Synthesis and crystal structure of aqua(diaminobithiazole) (iminodiacetato)nickel(II) hydrate. J. Coord. Chem., 58: 735–740.
112. Ahn, J.-W., Jang, K. H., Yang, H.-C., Oh, K.-B., Lee, H.-S., Shin, J. (2007) Bithiazole metabolites from the Myxobacterium *Myxococcus fulvus*. Chem. Pharm. Bull., 55: 477–479.
113. Suzuki, Y., Ojika, M., Sakagami, Y., Fudou, R., Yamanaka, S. (1998) Cystothiazoles C-F, new bithiazole-type antibiotics from the myxobacterium *Cystobacter fuscus*. Tetrahedron, 54: 11399–11404.
114. Sasse, F., Böhlendorf, B., Hermann, M., Kunze, B., Forche, E., Steinmetz, H., Höfle, G., Reichenbach, H. (1999) Melithiazols, new β-methoxyacrylate inhibitors of the respiratory chain isolated from Myxobacteria. J. Antibiot., 52: 721–729.
115. Weissman, K. J., Müller, R. (2010) Myxobacterial secondary metabolites: bioactives and modes-of-action. Nat. Prod. Rep., 27: 1276–1295.
116. Colon, A., Hoffman, T. J., Gebauer, J., Dash, J., Rigby, J. H., Arseniyadis, S., Cossy, J. (2012) Catalysis-based enantioselective total synthesis of myxothiazole Z, (14*S*)-melithiazole G and (14*S*)-cystothiazole F. Chem. Commun., 48: 10508–10510.

117. Williams, D. R., Patnaik, S., Clark, M. P. (2001) Total synthesis of cystothiazoles A and C. J. Org. Chem., 66: 8463–8469.
118. Quadri, L. E. N., Keating, T. A., Patel, H. M., Walsh, C. T. (1999) Assembly of the *Pseudomonas aeruginosa* nonribosomal peptide siderophore pyochelin: *in vitro* reconstitution of aryl-4,2-bisthiazoline synthetase activity from PchD, PchE, and PchF. Biochemistry, 38: 14941–14954.
119. Brandel, J., Humbert, N., Elhabiri, M., Schalk, I. J., Mislin, G. L. A., Albrecht-Gary, A.-M. (2012) Pyochelin, a siderophore of *Pseudomonas aeruginosa*: Physiochemical characterization of the iron(III), copper(II) and zinc(II) complexes. Dalton Trans., 41: 2820–2834.
120. Hare, N. J., Soe, C. Z., Rose, B., Harbour, C., Codd, R., Manos, J., Cordwell, S. J. (2012) Proteomics of *Pseudomonas aeruginosa* Australian epidemic strain 1 (AES-1) cultured under conditions mimicking the cystic fibrosis lung reveals increased iron acquisition via the siderophore pyochelin. J. Proteome Res., 11: 776–795.
121. Chen, Z.-F., Tan, M.-X., Liu, L.-M., Liu, Y.-C., Wang, H.-S., Yang, B., Peng, Y., Liu, H.-G., Liang, H., Orvig, C. (2009) Cytotoxicity of the traditional chinese medicine (TCM) plumbagin in its copper chemistry. Dalton Trans., 10824–10833.
122. Padhye, S., Dandawate, P., Yusufi, M., Ahmad, A., Sarkar, F. H. (2012) Perspectives on medicinal properties of plumbagin and its analogs. Med. Res. Rev., 32: 1131–1158.
123. Quinoa, E., Adamczeski, M., Crews, P., Bakus, G. J. (1986) Bengamides, heterocyclic anthelmintics from a Jaspidae marine sponge. J. Org. Chem., 51: 4494–4497.
124. Towbin, H., Bair, K. W., DeCaprio, J. A., Eck, M. J., Kim, S., Kinder, F. R., Morollo, A., Mueller, D. R., Schindler, P., Song, H. K., van Oostrum, J., Versace, R. W., Voshol, H., Wood, J., Zabludoff, S., Phillips, P. E. (2003) Proteomics-based target identification: bengamides as a new class of methionine aminopeptidase inhibitors. J. Biol. Chem., 278: 52964–52971.
125. Lu, J.-P., Yuan, X.-H., Yuan, H., Wang, W.-L., Wan, B., Franzblau, S. G., Ye, Q.-Z. (2011) Inhibition of *Mycobacterium tuberculosis* methionine aminopeptidase by bengamide derivatives. ChemMedChem, 6: 1041–1048.
126. Newman, D. J., Cragg, G. M. (2012) Natural products as sources of new drugs over the 30 years from 1981–2010. J. Nat. Prod., 75: 311–335.
127. Lam, K. S. (2007) New aspects of natural products in drug discovery. Trends Microbiol., 15: 279–289.
128. Garson, M. J. (1993) The biosynthesis of marine natural products. Chem. Rev., 93: 1699–1733.
129. Demain, A. L. (1999) Pharmaceutically active secondary metabolites of microorganisms. Appl. Microbiol. Biotechnol., 52: 455–463.
130. Ganesan, A. (2008) The impact of natural products upon modern drug discovery. Curr. Opin. Chem. Biol., 12: 306–317.
131. Ming, L.-J. (2003) Structure and function of metalloantibiotics. Med. Res. Rev., 23: 697–762.
132. Priuska, E. M., Clark-Baldwin, K., Pecoraro, V. L., Schacht, J. (1998) NMR studies of iron-gentamycin complexes and the implications for aminoglycoside toxicity. Inorg. Chim. Acta, 273: 85–91.

133. Gaggelli, E., Gaggelli, N., Valensin, D., Valensin, G., Jeżowska-Bojczuk, M., Kozłowski, H. (2002) Structure and dynamics of the lincomycin-copper(II) complex in water solution by ^{1}H and ^{13}C NMR studies. Inorg. Chem., 41: 1518–1522.
134. Porath, J., Hansen, P. (1991) Cascade-mode multiaffinity chromatography: fractionation of human serum proteins. J. Chromatogr., 550: 751–764.
135. Kuehnbaum, N. L., Britz-McKibbin, P. (2013) New advances in separation science for metabolomics: resolving chemical diversity in a post genomic era. Chem. Rev., 113: 2437–2468.
136. Patti, G. J., Yanes, O., Siuzdak, G. (2012) Innovation metabolomics: the apogee of the omics trilogy. Nat. Rev. Mol. Cell Biol., 13: 263–269.
137. Johnson, C. H., Gonzalez, F. J. (2012) Challenges and opportunities of metabolomics. J. Cell. Physiol., 227: 2975–2981.
138. Mounicou, S., Szpunar, J., Lobinski, R. (2009) Metallomics: the concept and methodology. Chem. Soc. Rev., 38: 1119–1138.
139. Kersten, R. D., Dorrestein, P. C. (2009) Secondary metabolomics: Natural products mass spectrometry goes global. ACS Chem. Biol., 4: 599–601.
140. Rochfort, S. (2005) Metabolomics reviewed: a new "omics" platform technology for systems biology and implications for natural products research. J. Nat. Prod., 68: 1813–1820.
141. Phelan, V. V., Liu, W.-T., Pogliano, K., Dorrestein, P. C. (2012) Microbial metabolic exchange - the chemotype-to-phenotype link. Nat. Chem. Biol., 8: 26–35.
142. Ryan, D., Robards, K. (2006) Metabolomics: The greatest omics of them all? Anal. Chem., 78: 7954–7958.
143. Thiericke, R., Rohr, J. (1993) Biological variation of microbial metabolites by precursor-directed biosynthesis. Nat. Prod. Rep., 10: 265–289.
144. Bode, H. B., Bethe, B., Hofs, R., Zeeck, A. (2002) Big effects from small changes: possible ways to explore nature's chemical diversity. ChemBioChem, 3: 619–627.
145. Meiwes, J., Fiedler, H.-P., Zähner, H., Konetschny-Rapp, S., Jung, G. (1990) Production of desferrioxamine E and new analogues by directed fermentation and feeding fermentation. Appl. Microbiol. Biotechnol., 32: 505–510.
146. Ankenbauer, R. G., Staley, A. L., Rinehart, K. L., Cox, C. D. (1991) Mutasynthesis of siderophore analogues by *Pseudomonas aeruginosa*. Proc. Natl. Acad. Sci. USA, 88: 1878–1882.
147. Tschierske, M., Drechsel, H., Jung, G., Zähner, H. (1996) Production of rhizoferrin and new analogues obtained by directed fermentation. Appl. Microbiol. Biotechnol., 45: 664–670.
148. Soe, C. Z., Pakchung, A. A. H., Codd, R. (2012) Directing the biosynthesis of putrebactin or desferrioxamine B in *Shewanella putrefaciens* through the upstream inhibition of ornithine decarboxylase. Chem. Biodivers., 9: 1880–1890.
149. Ledyard, K. M., Butler, A. (1997) Structure of putrebactin, a new dihydroxamate siderophore produced by *Shewanella putrefaciens*. J. Biol. Inorg. Chem., 2: 93–97.
150. Capon, R. J. (2012) Biologically active natural products from Australian marine organisms, in: Tringali, C. (ed.) *Bioactive Compounds from Natural Sources*, pp. 579–602 (Boca Raton, FL, CRC Press).

151. Kim, T. K., Garson, M. J., Fuerst, J. A. (2005) Marine actinomycetes related to the 'Salinospora' group from the Great Barrier Reef sponge *Pseudoceratina clavata*. Environ. Microbiol., 7: 509–518.
152. Udwary, D. W., Zeigler, L., Asolkar, R. N., Singan, V., Lapidus, A., Fenical, W., Jensen, P. R., Moore, B. S. (2007) Genome sequencing reveals complex secondary metabolome in the marine actinomycete *Salinispora tropica*. Proc. Natl. Acad. Sci., USA, 104: 10376–10381.
153. Harvey, C. J. B., Publisi, J. D., Pande, V. S., Cane, D. E., Khosla, C. (2012) Precursor-directed biosynthesis of an orthogonally functional erythromycin analog: selectivity in the ribosome macrolide binding pocket. J. Am. Chem. Soc., 134: 12259–12265.
154. Lifa, T., Ejje, N., Codd, R. (2012) Coordinate-bond-dependent solid-phase organic synthesis of biotinylated desferrioxamine B: A new route for metal-specific probes. Chem. Commun., 48: 2003–2005.
155. Hou, Y., Braun, D. R., Michel, C. R., Klassen, J. L., Adnani, N., Wyche, T. P., Bugni, T. S. (2012) Microbial strain prioritization using metabolomics tools for the discovery of natural products. Anal. Chem., 84: 4277–4283.
156. Boughton, B. A., Callahan, D. L., Silva, C., Bowne, J., Nahid, A., Rupasinghe, T., Tull, D. L., McConville, M. J., Bacic, A., Roessner, U. (2011) Comprehensive profiling and quantitation of amine group containing metabolites. Anal. Chem., 83: 7523–7530.
157. Boettcher, T., Pitscheider, M., Sieber, S. A. (2010) Natural products and their biological targets: Proteomic and metabolomic labeling strategies. Angew. Chem., Int. Ed., 49: 2680–2698.
158. Carlson, E. E. (2010) Natural products as chemical probes. ACS Chem. Biol., 5: 639–653.
159. Visca, P., Imperi, F., Lamont, I. L. (2007) Pyoverdine siderophores: From biogenesis to biosignificance. Trends Microbiol., 15: 22–30.
160. Lamont, I. L., Beare, P. A., Ochsner, U., Vasil, A. I., Vasil, M. L. (2002) Siderophore-mediated signaling regulates virulence factor production in *Pseudomonas aeruginosa*. Proc. Natl. Acad. Sci. USA, 99: 7072–7077.
161. Meyer, J.-M., Van, V. T., Stintzi, A., Berge, O., Winkelmann, G. (1995) Ornibactin production and transport properties in strains of *Burkholderia vietnamiensis* and *Burkholderia cepacia* (formerly *Pseudomonas cepacia*). BioMetals, 8: 309–317.
162. Sharman, G. J., Williams, D. H., Ewing, D. F., Ratledge, C. (1995) Determination of the structure of exochelin MN, the extraceullular siderophore from *Mycobacterium neoaurum*. Chem. & Biol., 2: 553–561.
163. Dhungana, S., Miller, M. J., Dong, L., Ratledge, C., Crumbliss, A. L. (2003) Iron chelation properties of an extracellular siderophore exochelin MN. J. Am. Chem. Soc., 125: 7654–7663.
164. Sheldon, R. A. (2005) Green solvents for sustainable organic synthesis: state of the art. Green Chem., 7: 267–278.
165. Cue, B. W., Zhang, J. (2009) Green process chemistry in the pharmaceutical industry. Green Chem. Lett. Rev., 2: 193–211.

166. Sheldon, R. A. (2007) The E factor: fifteen years on. Green Chem., 9: 1273–1283.
167. Umezawa, H., Suhara, Y., Takita, T., Maeda, K. (1966) Purification of bleomycins. J. Antibiot., 19: 210–215.
168. Gupta, M., Caniard, A., Touceda-Varela, A., Campopiano, D. J., Mareque-Rivas, J. C. (2008) Nitrilotriacetic acid-derivatized quantum dots for simple purification and site-selective fluorescent labeling of active proteins in a single step. Bioconjugate Chem., 19: 1964–1967.